LIFE SCIENCES

# Hunting bats adjust their echolocation to receive weak prey echoes for clutter reduction

**Laura Stidsholt[1]*, Stefan Greif[2,3], Holger R. Goerlitz[3], Kristian Beedholm[1], Jamie Macaulay[1], Mark Johnson[4], Peter Teglberg Madsen[1]**



**How animals extract information from their surroundings to guide motor patterns is central to their survival. Here, we use echo-recording tags to show how wild hunting bats adjust their sensory strategies to their prey and natural environment. When searching, bats maximize the chances of detecting small prey by using large sensory volumes. During prey pursuit, they trade spatial for temporal information by reducing sensory volumes while increasing update rate and redundancy of their sensory scenes. These adjustments lead to very weak prey echoes that bats protect from interference by segregating prey sensory streams from the background using a combination of fast-acting sensory and motor strategies. Counterintuitively, these weak sensory scenes allow bats to be efficient hunters close to background clutter broadening the niches available to hunt for insects.**

## INTRODUCTION

Hunting predators must find, pursue, and catch often fast-moving prey among myriad distracting sensory cues. Solving this sensorimotor challenge requires rapid changes in sensory attention and in motor outputs in response to both prey and environment (*1*). Insectivorous bats rely on echolocation to orient and catch prey on the wing under conditions of poor lighting (*2*), and their call patterns reveal the dynamic sensory strategies adopted to hunt successfully. During foraging, they typically follow a three-phased biosonar strategy comprising search, approach, and capture (feeding buzz) phases (audio S1). This model for how bats use echolocation to track and capture prey is based largely on laboratory experiments (*3*–*6*) and ground-based snapshot recordings in the wild as bats fly past stationary microphone arrays or cameras (*7*, *8*). Laboratory experiments have revealed that echolocating bats can adjust both their echolocation signals (*9*, *10*) and their flight trajectories (*11*, *12*) to reduce acoustic background clutter when hunting or solving tasks. Much less is known about the way these adjustments are used in wild foraging where echoes return from multiple objects in different directions, creating complex acoustic scenes that require rapid auditory identification, grouping, and tracking of individual echo streams to inform prey interception. Here, we use high-resolution on-board echo- and motion-recording tags to quantify how bats adjust their sensory sampling and motor strategies when hunting aerial prey in clutter and in open space in the wild. Specifically, we sought to test the hypotheses that wild greater mouse-eared bats (i) trade sensory volumes for update rates to successfully intercept evasive aerial prey, (ii) rely on stereotyped movement patterns to enable fast motor responses during aerial prey capture, and (iii) actively seek to maximize echo information from small prey to aid auditory processing via sensory and motor adjustments.

[1]Zoophysiology, Department of Biology, Aarhus University, Aarhus, Denmark. [2]Department of Zoology, Tel Aviv University, Tel Aviv, Israel. [3]Acoustic and Functional Ecology, Max Planck Institute for Ornithology, Seewiesen, Germany. [4]Aarhus Institute of Advanced Studies, Aarhus University, Aarhus, Denmark.
*Corresponding author. Email: laura.stidsholt@bio.au.dk

## RESULTS AND DISCUSSION

### Sensory volumes traded for update rates

To investigate the sensorimotor dynamics of wild bats, we equipped 10 female greater mouse-eared bats (*Myotis myotis*) in Bulgaria with miniature biologging tags (*13*) that recorded synchronously the movement patterns, echolocation calls and returning echoes from aerial prey, and surroundings during a full night of foraging. The tagged bats ($n = 10$; table S1) were released after dusk and commuted to night-time foraging sites, where they gleaned insects off the ground (indicated by distinct motor patterns in the acceleration data) or caught prey in midair (indicated by emission of feeding buzzes in flight) before returning to the roost before dawn (Supplementary Materials and table S2). The bats used echolocation to detect and pursue aerial prey, transitioning through search, approach, and capture phases, during which the vocal output and corresponding sensory volumes changed markedly along with the returning echoic scene and motor patterns (Fig. 1; see summary values for all bats in Fig. 2; movies S1 and S2). We analyzed 457 aerial captures of which 371 were successful (indicated by audible chewing sounds after each feeding buzz). In the search phase, the bats emit powerful calls (Fig. 2A) with large and variable sensory volumes (fig. S7) (*14*) of 0.07 to 21.1 $m^3$ (95% data range) for typical prey targets [wingspans from 5 mm (e.g., Diptera) to 50 mm (e.g., Lepidoptera)] (Fig. 2D) to maximize chances of prey detection. The large sensory volumes in the search phase highlight that wild bats generally seek to maximize the chances of detecting aerial prey by using intense calls and that they can dynamically adjust these volumes to the acoustic scenes encountered.

To efficiently track detected prey, the bats, on average, transition into the approach phase (inferred from reductions in call intervals and source levels) at 0.42 s (±0.15 SD) before prey capture. This confirms earlier observations that bats hunting in the wild have less than 500 ms between detection and capture of prey (*7*). Despite a 10-fold reduction in mean sensory volumes from search to approach phase (Figs. 1C and 2D), the spatial redundancy [i.e., the number of times the bat ensonifies the same volume of air while flying forward (fig. S10)] remains constant (Fig. 2E) because the repetition rate increases (Fig. 2B). In contrast, as the bats transition into the buzz phase, the redundancy doubles (Fig. 2E) because of very high

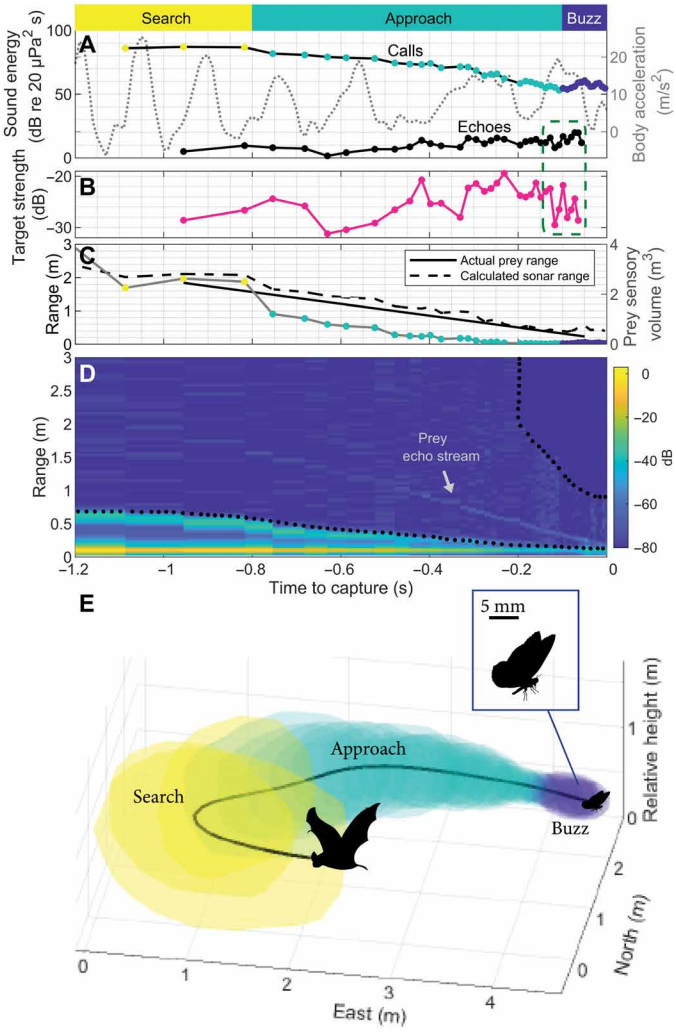


**Fig. 1. Bats adjust their vocalizations to receive unmasked prey echoes from gradually smaller sensory volumes to guide prey capture.** (**A**) During the chase, the bat reduces the outgoing energy (colored dots) of its calls by ~40 dB and increases call repetition rate. Returning prey echoes (black) are very weak and cover a dynamic range of ~20 dB. Wingbeats (gray line) were derived from oscillations in the body acceleration. (**B**) The estimated target strength (TS) of the prey insect fluctuates between −30 and −20 dB at 0.1 m. The fast fluctuations in TS and EL at the end of the chase (green dashed box) are probably caused by wingbeats from the prey. (**C**) The measured range of the bat to the prey is shorter than the estimated maximum range over which the bat can hear the insect (dashed black lines). The sensory volumes of each call decrease during the capture (gray lines). (**D**) The echogram visualizes the sensory scene during the capture. Here, the prey echo stream consisting of ~35 echoes is clearly visible during the entire last second of the chase. The bat approaches the insect with a constant speed of 1.8 m/s in an open environment, as no clutter echoes are recorded by the tag. The dashed black lines mark the zone between two consecutive calls where the bat listens for returning echoes, i.e., the overlap free zone. (**E**) The dead-reckoned track (black line) and the calculated sensory volumes [colored shapes marking the three phases from (A): search, approach, and buzz] show how the bat maneuvers and adjusts its sensory volume to capture the insect (movie S2).

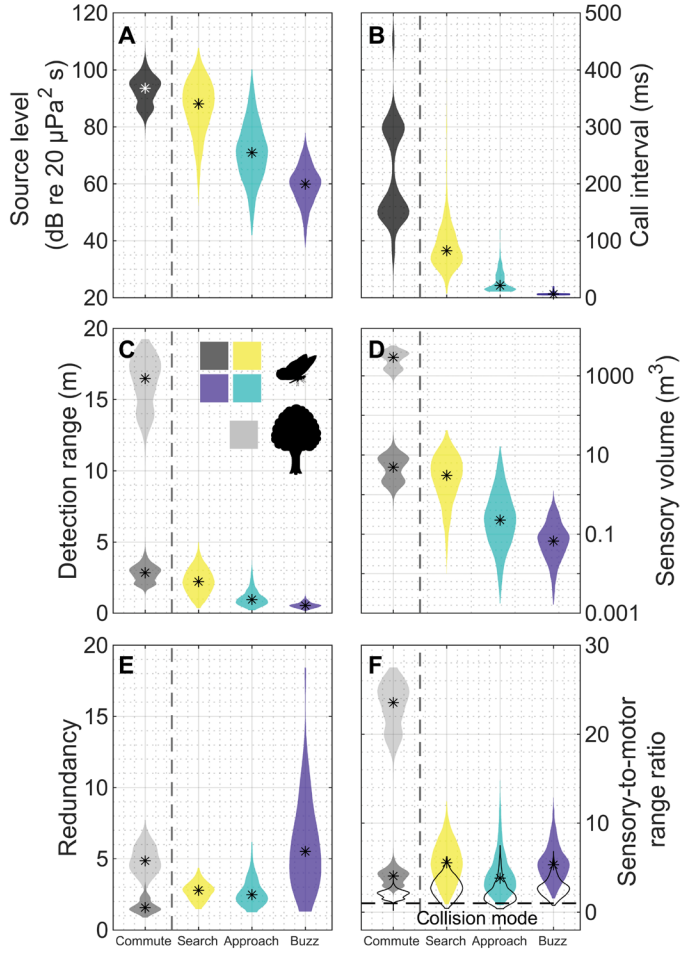


**Fig. 2. Bats switch from a deliberate to a reactive sensorimotor mode upon prey detection.** (**A** to **E**) Bats actively adjust their biosonar parameters to different targets (i.e., prey or large background structures such as a tree) (A and B) to regulate the detection distance (C), sensory volume (D), and spatial redundancy (E) during commuting flight and three stages of aerial capture. (**F**) The sensory-to-motor range ratio is the relationship between the detection range (C) and reaction range of the bats using a reaction time of 100 ms (solid violins) or 200 ms (black outline violins). All plots depict the *k* means distribution (shaded area) and means (stars) of the data. $n = 10$ bats, 121 captures (4 to 15 random prey captures per individual to balance the study because the individual bats attack prey between 4 and 103 times per night), 4562 foraging calls, and 4092 commuting calls.

repetition rates (Fig. 2B) despite the more than 45-fold drop in prey sensory volume down to 0.005 to 0.46 $m^3$ (95% data range; Fig. 2D). Thus, only before capturing the prey, bats narrow their acoustic gaze to focus on a single echo stream from their prey target by using high-speed sampling of a small absolute sensory volume. The strategy of using high-resolution information of prey acquires at fast update rates seems to be functionally similar to how visually guided predators such as predatory swallows and diurnal raptors focus on the frontal area of their field of view (*15*) at high resolution (*16*).

## From deliberate to reactive sensory modes

It has been hypothesized that bats, because of their short inferred prey detection ranges and fast flight speeds, must use a highly reactive sensory-motor operation with little or no time between prey detection and required adjustments to flight patterns to successfully intercept prey. Here, we tested that hypothesis to investigate whether wild bats indeed use a rapid and less informed (i.e., reactive mode) or a slower and more informed (i.e., deliberate) sensory strategy when hunting (*14*).

When bats commute to/from their foraging sites, they emit high-intensity echolocation calls forming sensory volumes of 2800 $m^3$ (±1300 SD) (Fig. 2D) for large targets such as trees. Because the sensory range (16 m) is much larger than the motor response range (0.7 m) [i.e., the range over which bats can react based on a reaction time of 100 ms (*17*) and flight speed of 7 m/s], the bats operate at high (>>10) sensory-to-motor range ratios (SMRs) for landmarks (Fig. 2F). This means that bats have a comparatively long time for movement planning despite high flight speeds, indicating a deliberative sensory-motor mode (*14*) during commuting. In contrast, the detection ranges and sensory volumes for small prey (Fig. 2, C and D) are generally much smaller because of their much poorer target strength (TS) (poor backscattering) resulting in small spatial overlaps between successive beams (Fig. 2E). Hunting bats therefore have comparatively little time to react to sensory information returning from within small sensory volumes and operate in a highly reactive sensory-motor mode during all stages of aerial prey captures (low SMR of ~5 using flight speeds of 4, 2.5, and 1 m/s for search, approach, and capture phases, respectively; Fig. 2F).

Although the SMRs during prey interactions are approximately constant across all four stages (i.e., commute, search, approach, and buzz), the bats achieve this in different ways. During commuting flight, when bats opportunistically encounter prey, and during prey search, the bats operate with low information flow rates (Fig. 2B) but long prey detection ranges (Fig. 2C, dark gray and yellow) that can support fast flight speeds. Conversely, in the buzz phase, prey detection ranges are so small (<1 m) that a SMR > 1 [i.e., allowing some reaction to prey movements as opposed to a collision mode (*14*)] is only maintained by decreasing flight speed. This is in contrast to most other predators that operate at much higher SMRs (*18*, *19*) and therefore hunt in a more informed, deliberate sensory-motor mode, allowing for prey selection and planning of a greater range of complex motor patterns during most of the hunt (*14*).

We then tested the hypothesis that bats hunting in this highly reactive mode with a direct coupling between sensory input and necessary motor action rely on stereotyped movement patterns when catching aerial prey. To our surprise, we found large variations in the relative bat-prey approach speeds [1.4 to 4.9 m/s (95% data range), derived from the slopes of the echo streams; fig. S1], indicating that bats used nonstereotypic motor approaches when tracking prey with potentially different evasive strategies (*20*). Some of the typical aerial prey types targeted by greater mouse-eared bats belong in families with ears (e.g., *Geometridae*, *Notodontidae*, and *Noctuidae*), allowing these moths to perform evasive maneuvers. This shows that despite hunting over extremely short time scales, bats use versatile motor patterns that are supported by ultrafast echo-informed sensory-motor responses to catch evasive prey (*17*).

## Weak prey echoes in a simplified auditory scene

To successfully hunt prey in a reactive mode over short time scales, bats must rely on efficient stream segregation of echoes to guide their motor patterns (*1*). We hypothesized that bats actively shape their auditory scene to facilitate stream segregation by controlling the timing and level of their calls and, therefore, the relative timing and level of echoes from prey and background (*21*). To test this, we used echograms to visualize and quantify auditory streams of the bats while hunting ($n$ = 451 captures; see example capture in Fig. 1D). We show that the bats control their call timing to receive echoes in an overlap-free zone (i.e., a time window after the emitted call and before the next vocalization) (*22*, *23*) in which echo ranging is unambiguous (Fig. 1D, dashed black lines).

This confirms laboratory experiments suggesting that bats seek to place echoes of interest between their so-called outer and inner windows (*22*). It may be hypothesized that bats would seek to maximize the received echo levels from their small prey to be well above hearing thresholds to facilitate auditory streaming. However, despite a wide range of back-calculated TSs (at 0.1 m) (Fig. 3, A and B), the received aerial prey echo levels were consistently extremely low with a dynamic range of 5 to 29 dB re 20 $\mu Pa^2s$ (95% data range) for the echoes that we could extract (Fig. 3D, black) (fig. S6). The remaining echo streams (58%, 267 of 451 echo streams) were below the noise floor of the tag microphone, suggesting echolocation based on echo levels below 5 dB re 20 $\mu Pa^2s$ or 30 dB rms (root mean square).

Bats have been reported to have echo detection thresholds from 0 (*24*) to 55 dB re 20 Pa (*25*) in laboratory experiments. Here, we show that wild greater mouse-eared bats echolocate prey for capture using echo levels that are only of use to them if they have an acute hearing sensitivity. This sensitivity must exceed the sensitivity reported for many bats in the laboratory but can be supported by auditory sensitivities comparable to those of gleaning bats (down to −27 to −39 dB re 20 $\mu Pa^2s$, using an integration time of 125 ms) (*26*, *27*) and nocturnal predators such as owls and cats that have similarly evolved very sensitive hearing (−26 to −27 dB re 20$\mu Pa^2s$, using a 100-ms signal duration) (*28*, *29*).

Thus, bats deliberately only use the lowest part of their auditory dynamic range for processing of prey echoes by actively reducing their call levels during approach and capture (Fig. 3). This raises the

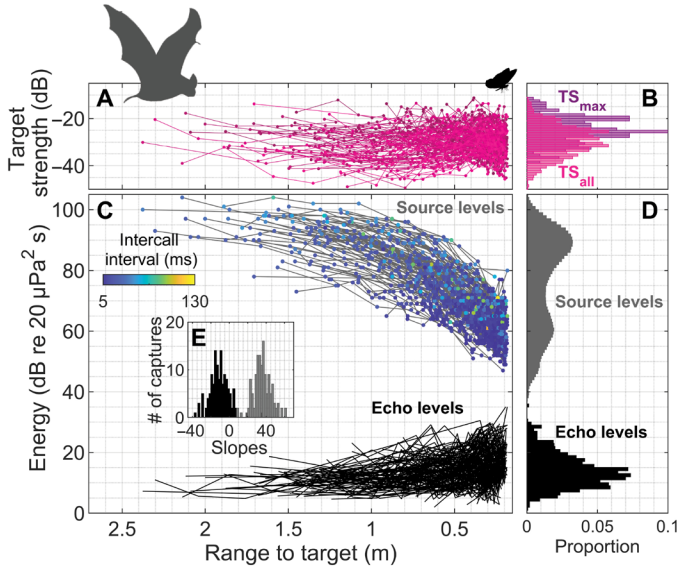


**Fig. 3. Hunting bats actively generate weak prey echoes from a large range of prey items.** (**A** and **B**) Estimated TSs of aerial prey vary over a dynamic range of approximately 30 dB. (**C** and **D**) Source levels (gray) and prey echo levels (black) change as bats approach their target. (A to C) $n$ = 1387 calls, 204 captures with visible prey echoes. (D) $n$ = 10 bats; 43 recording hours; 1,200,368 calls; 1387 echoes. (**E**) Distribution of the slope for the distance-dependent change in source level (gray) and received echo level (black). Source levels followed a logarithmic fit to target range with a slope of 29 dB (±11 SD; $R^2$ = 0.79); echo levels followed a slope of −10 dB (±10 SD; $R^2$ = 0.35). $n$ = 123 captures. This means that call source levels reduce by an average of 8.7 dB [i.e., 29*$\log_{10}(2)$] per halving of distance while echo levels tend to increase by 3 dB over the same distance.

question of why bats opt for such weak echoes spanning a relatively low echo dynamic range if they can increase echo levels for auditory processing by producing louder calls. At long ranges, call intensity may already be maximized (*30*), and the low echo strength is a consequence of small prey items and high absorption of ultrasound in air. However, as wild bats approach their prey, they produce calls that are well below their maximum intensity, resulting in extremely low echo levels close to the hearing threshold. Bats pursuing aerial prey in the laboratory decrease their output levels logarithmically with target range ($R$), roughly halving call source level for each halving of range [an intensity adjustment of ~ $-20\log_{10}(R)$ dB] (*31*–*33*). This compensates for about half of the decreasing acoustic propagation loss as targets are approached, resulting in echo levels that double for every halving in range, presumably to avoid very loud echoes when approaching prey (*34*). Our wild bats actively lower the energy of their calls over the course of captures by ~30 dB (Fig. 3C) corresponding to an average logarithmic decrease of 29 (±12) dB per decade of reduction in range to prey (Fig. 3E, gray). This leads to consistently weak but increasing echo levels of 10 dB (±10) per decade of reduction in range to prey (Fig. 3, C and D, black) across all prey ranges (Fig. 3, A and B). Over the course of a capture, echo levels therefore generally increase but with large variations likely caused by both the fluctuating TSs from insect wing movements and the use of different call source levels for the same ranges (Fig. 3A).

Thus, wild bats hunting small prey reduce their source levels markedly when within 2 m of their prey to consistently receive weak echo levels across all prey ranges that are sufficient for auditory processing but that fall in an unexpectedly low and narrow distribution just above their hearing threshold. These results support the recent suggestion that bats use a dynamic range compression strategy (*35*) to avoid receiving loud echoes (*36*) and perhaps in concert with call-induced stapedial reflexes (*31*) to maintain a large number of neurons in a nonrefractory state available for auditory processing. To process these weak echoes, bats may have dedicated a large part of their auditory neurons to fire at low levels (*37*) so as to maximize detection volumes of small prey despite low-intensity calls and, hence, to maximize time to execute complex motor plans for capture. We consequently posit that bats actively adjust call levels during close approaches to keep prey echo levels in a fairly narrow dynamic range close to their hearing thresholds that, in turn, maximizes the overall sensory-motor performance.

## Vocal and motor responses reduce clutter

An alternative driver for, or additional benefit of, using low source levels during approach and buzzing may be to minimize clutter from farther objects (fig. S3) that would otherwise complicate the auditory stream segregation of prey. To test that hypothesis and to uncover how bats hunt prey in such cluttered habitat, we first tracked clutter echo streams in echograms of aerial capture attempts and then compared the acoustic and movement behavior during captures both with (57% of the captures; $n$ = 260 of 457), and without, detectable clutter (fig. S2 and movie S2). Within the last 3 s before prey capture, prey echoes appear within about 2-m range of the bat, whereas clutter appears at up to 8-m range due to the higher TS of clutter-generating structures (Fig. 4). The clutter echoes disappeared just before prey capture [−0.4 s (±0.3 SD); Fig. 4B, gray], resulting in simplified auditory scenes during the final moments of prey capture. The continued presence of clutter echoes during the pursuit indicates that the tagged bats flew alongside large background objects, such as forest edges, at ranges of 1.9 to 7.8 m (Fig. 4). By keeping a minimum range to the clutter sources of about one prey detection range, the bats temporally separate clutter echo streams from the echoes of potential prey, thereby facilitating auditory stream segregation of the weaker prey echoes.

We next investigated how the source levels and flight paths varied before and after prey detection in the different habitats (cluttered versus uncluttered) to test whether bats use motor and sensory adjustments to aid in clutter rejection. Before prey detection (i.e., >2 s before captures), we found that bats increased call source levels, used less variable flight paths [GLMM (generalized linear mixed-effect model); $P < 0.01$, $R^2$ (coefficient of determination) = 0.6; table S3], and used longer call intervals ($t$ test; $t = -11.5$, $P < 0.001$) in cluttered versus uncluttered conditions. This is counter to what has been found in microphone array recordings in the wild where bats have been shown to call weaker (*38*, *39*) and at higher rates (*23*) to maintain sufficient updates to navigate in cluttered environments while avoiding range ambiguity. In contrast, the wild bats in our study emitted intense calls at slower rates perhaps to keep unambiguous clutter streams audible even in situations where the bats fly up to tens of meters away from background structures (Fig. 4), while still retaining overlap between successive sensory volumes (Fig. 2E).

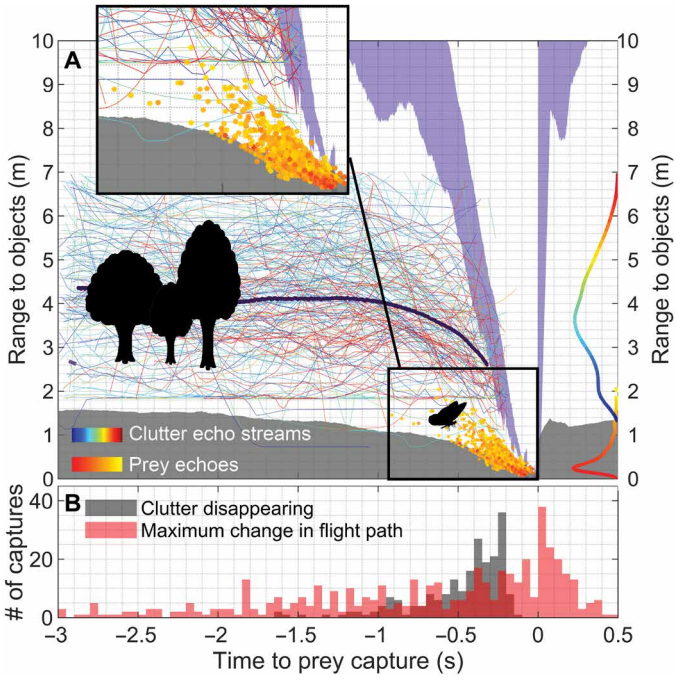


**Fig. 4. Bats separate prey and clutter echo streams by acoustic gaze and motor pattern adjustments.** (**A**) The durations of the current call and the following call determine the inner (gray) and outer (purple) window, which together determine the overlap-free perceptual zone. The echo streams of prey (colored dots) and clutter (colored lines, according to each individually tagged bat; the black line depicts mean clutter distance) are located within the overlap-free zone. Histograms on the right axis show that prey and clutter echoes are spatially separated. (**B**) Timing of the disappearance of clutter from the auditory scenes (gray) and the maximum change in the flight path (red). The bats approach their prey with flexible nonstereotypic flight patterns, as their maximum change in flight paths span a large time scale (~2 s).

We thus argue that bats searching for prey actively keep clutter streams in their auditory scenes by maintaining long call intervals and large sensory volumes to use clutter as echo acoustic flow (*40*, *41*) or as a spatial anchor for navigation. Furthermore, this sensory strategy maintains long detection ranges and therefore allows time for reactions while avoiding range ambiguity. Thus, in search and approach phases, the bats operate at a high sensory-to-motor ratio and therefore likely plan the motor patterns necessary to maximize detection of prey against clutter and to intercept their prey.

During the last stage of prey capture, clutter echoes disappeared just before prey capture [−0.4 s (±0.3 SD); Fig. 4B, gray], resulting in even simpler auditory scenes close to prey interception. The vocal and motor patterns when hunting in open space or in cluttered habitats at this stage remained the same. This suggests that the mean $29\log_{10}(R)$ reduction in call source levels (Figs. 3 and 4) is sufficient to eliminate interference from clutter only before interception (i.e., on average over the last 0.4 s before prey capture; Fig. 4B, gray). Furthermore, at this late stage in the capture, the bat's movement is likely dominated by maneuvering to intercept prey and not to avoid collision with large background structures: In the absence of clutter echoes, collision avoidance must be achieved by spatial memory rather than sensory feedback. This result suggests that the motor patterns have already been planned at an earlier stage further supporting our notion that bats operate in a highly reactive sensory mode (Fig. 2F) close to prey capture.

Thus, we conclude that adjustments of both sensory (vocal) and motor (flight trajectory) patterns at an early stage of the hunt increase the efficiency of prey capture in complex environments. This strategy serves both to counter insects that seek refuge in vegetation as a predator-abatement strategy and to expand the niches available to foraging bats.

In conclusion, we found that bats actively adjust call intensity to generate weak prey echoes with a low dynamic range. This may be a consequence of gaze adjustments aimed at simplifying the natural auditory scene, thereby easing tracking of prey echo streams in cluttered environments.

These results show how wild bats adjust their sensory sampling and flight motor planning during foraging so as to separate clutter and prey sensory streams in time and space. Doing so may critically facilitate perceptual organization of their sensory inputs to inform echo-guided captures in less than 0.5 s. Bats are therefore extreme examples of predators that have evolved a flexible and rapid control over their dominant sensory system and motor actions to hunt fast, evasive prey efficiently in highly dynamic and complex scenes.

## MATERIALS AND METHODS

### Experimental procedure

All experiments were carried out under the following licenses: 721/12.06.2017, 180/07.08.2018, and 795/17.05.2019 from MOEW (Ministry of Environment and Water)–Sofia and RIOSV (Regional Inspectorate of Environment and Waters)–Ruse. During the field seasons of 2017, 2018, and 2019, we tagged and recaptured 10 female *M. myotis* with on-board sound and movement tags. The acoustic tag used for these studies recorded audio with a Knowles ultrasonic microphone (FG-23329) and sampled the bat's behavior by synchronized triaxial accelerometers and magnetometers. The audio was recorded at a sample rate of 187.5 kHz (16 bit) and a clip level of 121 dB re 20 μPa. A one-pole, 10-kHz high-pass filter and an anti-aliasing filter of 80 kHz were filtering the output of the microphone. The accelerometers were sampled at 1000 Hz (16 bit, 8 g) with a 250 Hz anti-alias filter, while the magnetometers were sampled at 50 Hz. The tags weighed between 3.5 and 3.9 g including radio transmitters to locate the bats (table S1).

The bats were caught with a harp trap at Orlova Chuka cave, close to Ruse, North east Bulgaria, in the early mornings as they returned to the roost. The bats were kept at the Siemers Bat Research Station in Tabachka to measure the forearm lengths, CM3, and body weights (table S1). Bats weighing above 29 g were tagged and released the following night between 10 and 11 p.m. at a field 8 km from the roost (decimal degrees, 43.622097 and 25.864917). The tags were wrapped in balloons for protection and glued to the fur on the back between the shoulders with skin bond latex glue (Ostobond). The bats on average spend 2 to 14 days equipped with the tags until we recaptured the bats at the cave or until the tags were detached from the bats and fell to the ground below the colony. Upon recapture, the bats were weighed and checked for any sign of discomfort from the tagging before they were released back to the colony.

The tags weighed 11 to 14% of the body mass of the bats, which is higher than the 5% rule. The bats on average lost ~2.5 g during the tagging, which is less than the average diurnal loss in body mass of 5.5 g during the 1 day spent at the station before release (table S1). In addition, these bats caught prey up to several hundred times per night with high success rates (table S2), indicating that the tags did not have large, if any, effects on their ability to maneuver and catch prey (*42*). The bats were weighed and inspected after instrumentation for any sign of discomfort before they were released back to the colony.

### Categorization of behaviors

All wild tag recordings were manually analyzed by displaying both the acoustic and the inertial sensor data in 7-s segments with an additional option of playing back audio data. The visualization included three separate windows with synchronized data: an envelope of audio data filtered by a 20-kHz four-pole high-pass filter to detect the echolocation calls. A spectrogram of audio data filtered by a 1-kHz one-pole high pass filter to visualize the full-bandwidth acoustic scene showing echolocation calls, conspecific calls, chewing sounds, wind noise, etc. The final window showed triaxial accelerometer and magnetometer data aiding the identification of wingbeats, landings, etc. Aerial capture attempts were identified in the wild data by comparison to the data from the prey capture study in the flight room. An aerial prey capture attempt was marked if the bat was flying both before and after a buzz.

The aerial captures were divided into search, approach, and buzz phases. The buzz phase was defined as the time interval where all call intervals were below 10 ms. In this study, we used the end of the buzz as the time of prey capture. The approach phases were defined by five participants manually marking the beginning of the approach phase based on call intervals and source levels plotted against time to prey capture. Whenever three of the five participants marked the transition into the approach phase in the same time interval (±120 ms), the mean value was used as the onset of the approach phase. The onset of the approach phase was on average 0.42 s (±0.15 SD) before prey capture. The approach phase ended when the first call was below 10 ms, indicating that the bat had transitioned into the buzz phase. We used the last 10 calls before the approach for analyzing search phase behaviors.

To compare the aerial captures to another operational mode (spatial orientation), we identified 100 s of each tag recording, where the bat was performing "commuting flight." This was defined as a time period with no prey capture attempts, regular flight pattern, a wingbeat frequency between 6 and 7 Hz, and stable output levels.

### Biosonar parameters

All calls in the tag recordings were automatically detected by a call detector and visually inspected to ensure correct extractions. Call energy of the off-axis calls (AOLs) were estimated in energy flux density (EFD) over a −6-dB energy window. The 14-dB offset between AOLs and source levels in the target approach experiment (fig. S4) was added to AOLs to estimate source levels from the onboard recordings. On the basis of the technique developed from the aerial prey captures in the flight room, we tracked echo streams on all echograms of the aerial captures to extract echo levels (ELs) and the range to target, *R* (figs. S5 and S6). The beginning and end of the prey echo streams were manually marked. The parameters, SL, EL, and *R*, were used to calculate TS at 0.1 m of the insect for each call-echo pair. The slope of the tracked prey echo streams corresponded to the speed at which the bat was homing in on the insect (i.e., the approach speed). The tagged bats in this study used approach speeds between 1.4 and 4.9 m/s (95% data range) (fig. S4). It was only possible to detect echo streams from the echograms in 45% of all the captures ($n$ = 204 of 457), meaning that we could only extract approach speeds from half of the captures.

### Clutter extractions

To understand how clutter interferes with prey captures, clutter echo streams from the surroundings were identified and tracked on the echograms. Clutter echoes were distinguished from prey echoes based on the time over which they returned. Large clutter echoes from, e.g., vegetation, return over a longer time interval compared to the single prey echoes from small aerial prey (fig. S4). The clutter detector was tracking the closest stream of echoes above a threshold of 0.5% of the maximum amplitude in a time window from 3 s to 200 ms before the beginning of the buzz and above a distance corresponding to the length of the call in meters in front of the bat to the next call emission.

A tracked echo stream was as categorized as a clutter echo stream if these two criteria were fulfilled:

1) More than six echoes were extracted in a sequence.

2) The distance to the reflecting object did not vary by more than 0.5 m from call to call. For two individuals, we set a 0.7-m threshold.

The range to clutter over successive calls was interpolated using cubic Hermite interpolation [pchip (MATLAB 2019a) to a sampling rate of 30 Hz] and smoothed with a moving mean of 0.16 s.

### Movement

We defined motor range as the minimum distance flown from sensory input until a motor reaction in response to this sensory input can occur. The motor range is calculated by multiplying the reaction time [100 ms (*17*) and 200 ms as a more conservative estimate, taking the processing time into account] with the velocity of the bat. Here, we used flight speeds of 7 m/s for commuting flights and 4, 2.5, and 1 m/s for the three different phases of foraging behavior, resulting in motor ranges of 0.7, 0.5, 0.25, and 0.1 m. The motor range was used to calculate SMRs. The three-dimensional flight paths of the bats were reconstructed by calculating the dead reckoning tracks (DRTs). The DRTs were calculated on the basis of the orientation of the bat recorded by the accelerometers and magnetometers and on assuming a flight speed for the bat (*43*). The accelerometer and magnetometer data were downsampled to a sample rate of 25 Hz and low-pass filtered by a delay free finite impulse response filter with a cutoff frequency of 3 Hz to reduce the high-frequency motion accelerations. This method is not accurate (*44*) but suitable to measure the relative angular changes in flight paths used in this study. The angular changes in the flight paths were measured every 40 ms (corresponding to every sample using a sample rate of 25 Hz) by calculating the vector between every successive samples of the DRT. The angle between two successive vectors was calculated for all data points along the flight path. To estimate the angular turns in a time interval over where the bats would likely be able to make a full reaction (reaction time between 80 and 120 ms), the angles were summed every 120 ms.

### Calculations of sensory volumes

To study how the changes in output level affected the spatial volume that the bat ensonified per call (i.e., the sensory volumes) and the number of times the same volume was ensonified (i.e., the sensory redundancy), we modeled the sensory beams per call along the three-dimensional flight path of the bats (figs. S7 to S10). The air volume that the bat ensonified per call varied according to source level, beam shape, hearing threshold, and the size of the target of interest. Here, we used source levels measured from on board the tag, the piston model to estimate the radiation pattern of the call, and a point target with TS of −30 dB at 0.1 m indicated from our recordings to model the prey sensory volume. To model the navigation sensory volumes, we chose a mirror target with TS of −10 dB for the commuting flights. We used a hearing threshold of 0 dB re 20 $\mu Pa^2s$, as we could observe acoustic reactions to echoes returning at and below this level in our field data.

### Statistical analysis

All statistical analyses were conducted using R version 4.0.3. We investigated the relationship between the presence of clutter in the auditory scenes of the bats and their acoustic and movement behavior. We used the presence of clutter as a response variable (hereafter named "clutter") and the change in source levels and flight paths as predictor variables (table S3) because laboratory studies have shown that bats adjust both the energy of their calls and their flight path when hunting in clutter. To explore this relationship, we tested the hypothesis that the presence of clutter in the echograms is explained by the slope of the six closest call source levels at 0.4 and 2 s before capture and by the maximum change in angle at 0.4 and 2 s before capture.

This time interval was chosen because the clutter on average disappeared 0.4 s before prey capture. We used the individual tagged animal (AnimalNo) as random effect.

We examined potential collinearity between predictor variables using variance inflation factors. No collinearity was found. After examining the response variable, we fitted a GLMM (glmer in R package "lme4") to the data using binomial distribution with a "logit" link. We used model selection procedures (dredge in R package "MuMIn") to examine the best-fitted model using the AICc (corrected Akaike information criterion). The best-fitted model included the maximum change in angle ($MA_{2sec}$) and the

slope of the call source levels ($SL_{2sec}$) at 2 s before capture. This was chosen as our best-fitted model. The residuals were examined and showed slight deviations from the expected distribution (using "simulateResiduals" in the "DHARMa" R package). The model was refit with a "cauchit" link function, which slightly improved the patterns.

Overall, the model including fixed and random effects explained 49% of the deviance in the clutter presence (using rsq in the "rsq" R package). Subtracting the random effect from the model decreased the explained deviance by 2%.

The effect of the individual predictor variables was examined (using R package "hier.part"). The change in source levels and flight path 2 s before capture explained 57 and 43%, respectively, of the deviance explained by the model. The best-fitted model (table S3) indicates that there is a significant effect of source level reductions and change in flight path on the presence of clutter in the auditory scenes of the bats before prey pursuit.

## SUPPLEMENTARY MATERIALS

Supplementary material for this article is available at http://advances.sciencemag.org/cgi/content/full/7/10/eabf1367/DC1

View/request a protocol for this paper from *Bio-protocol*.

## REFERENCES AND NOTES


1. M. S. Lewicki, B. Olshausen, A. Surlykke, C. F. Moss, Scene analysis in the natural environment. *Front. Psychol.* **5**, 199 (2014).
2. D. R. Griffin, Echolocation by blind men, bats and radar. *Science* **100**, 589–590 (1944).
3. A. Surlykke, C. F. Moss, Echolocation behavior of big brown bats, *Eptesicus fuscus*, in the field and the laboratory. *J. Acoust. Soc. Am.* **108**, 2419–2429 (2000).
4. L. Jakobsen, M. N. Olsen, A. Surlykke, Dynamics of the echolocation beam during prey pursuit in aerial hawking bats. *Proc. Natl. Acad. Sci. U.S.A.* **112**, 8119–8123 (2015).
5. D. R. Griffin, F. A. Webster, C. R. Michael, The echolocation of flying insects by bats. *Anim. Behav.* **8**, 141–154 (1960).
6. D. A. Cahlander, J. J. G. Mccue, F. A. Webster, The determination of distance by echolocating bats. *Nature* **201**, 544–546 (1964).
7. E. K. V. Kalko, Insect pursuit, prey capture and echolocation in pipestirelle bats (*Microchiroptera*). *Anim. Behav.* **50**, 861–880 (1995).
8. M. W. Holderied, C. Korine, M. B. Fenton, S. Parsons, S. Robson, G. Jones, Echolocation call intensity in the aerial hawking bat *Eptesicus bottae* (*Vespertilionidae*) studied using stereo videogrammetry. *J. Exp. Biol.* **208**, 1321–1327 (2005).
9. A. R. Wheeler, K. A. Fulton, J. E. Gaudette, R. A. Simmons, I. Matsuo, J. A. Simmons, Echolocating big brown bats, *Eptesicus fuscus*, modulate pulse intervals to overcome range ambiguity in cluttered surroundings. *Front. Behav. Neurosci.* **10**, 125 (2016).
10. B. Mao, M. Aytekin, G. S. Wilkinson, C. F. Moss, Big brown bats (*Eptesicus fuscus*) reveal diverse strategies for sonar target tracking in clutter. *J. Acoust. Soc. Am.* **140**, 1839–1849 (2016).
11. B. Falk, L. Jakobsen, A. Surlykke, C. F. Moss, Bats coordinate sonar and flight behavior as they forage in open and cluttered environments. *J. Exp. Biol.* **217**, 4356–4364 (2014).
12. M. Taub, Y. Yovel, Segregating signal from noise through movement in echolocating bats. *Sci. Rep.* **10**, 382 (2020).
13. L. Stidsholt, M. P. Johnson, K. Beedholm, L. Jakobsen, K. Kugler, S. Brinkløv, A. Salles, C. F. Moss, P. T. Madsen, A 2.6-g sound and movement tag for studying the acoustic scene and kinematics of echolocating bats. *Methods Ecol. Evol.* **10**, 48–58 (2019).
14. J. B. Snyder, M. E. Nelson, J. W. Burdick, M. A. MacIver, Omnidirectional sensory and motor volumes in electric fish. *PLOS Biol.* **5**, e301 (2007).
15. L. P. Tyrrell, E. Fernández-Juricic, The hawk-eyed songbird: Retinal morphology, eye shape, and visual fields of an aerial insectivore. *Am. Nat.* **189**, 709–717 (2017).
16. J. E. Boström, M. Dimitrova, C. Canton, O. Håstad, A. Qvarnström, A. Ödeen, Ultra-Rapid vision in birds. *PLOS ONE* **11**, e0151099 (2016).
17. C. Geberl, S. Brinkløv, L. Wiegrebe, A. Surlykke, Fast sensory–motor reactions in echolocating bats to sudden changes during the final buzz and prey intercept. *Proc. Natl. Acad. Sci.* **112**, 4122–4127 (2015).
18. D. M. M. Wisniewska, M. Johnson, J. Teilmann, L. Rojano-Doñate, J. Shearer, S. Sveegaard, L. A. A. Miller, U. Siebert, P. T. Madsen, Ultra-high foraging rates of harbor porpoises make them vulnerable to anthropogenic disturbance. *Curr. Biol.* **26**, 1441–1446 (2016).
19. J. Demšar, C. K. Hemelrijk, H. Hildenbrandt, I. L. Bajec, Simulating predator attacks on schools: Evolving composite tactics. *Ecol. Model.* **304**, 22–33 (2015).
20. T. Hügel, H. R. Goerlitz, Species-specific strategies increase unpredictability of escape flight in eared moths. *Funct. Ecol.* **33**, 1674–1683 (2019).
21. C. F. Moss, A. Surlykke, Auditory scene analysis by echolocation in bats. *J. Acoust. Soc. Am.* **110**, 2207–2226 (2001).
22. W. W. Wilson, C. F. Moss, Sensory-motor behavior of free-flying FM bats during target capture, in *Echolocation in Bats and Dolphins*, J. A. Thomas, C. F. Moss, M. Vater, Eds. (The University of Chicago Press, 2004), pp. 22–27.
23. E. K. V. Kalko, H.-U. Schnitzler, Plasticity in echolocation signals of European pipistrelle bats in search flight: Implications for habitat use and prey detection. *Behav. Ecol. Sociobiol.* **33**, 415–428 (1993).
24. S. A. Kick, Target-detection by the echolocating bat, *Eptesicus fuscus*. *J. Comp. Physiol.* **145**, 431–435 (1982).
25. C. F. Moss, J. A. Simmons, Acoustic image representation of a point target in the bat *Eptesicus fuscus*: Evidence for sensitivity to echo phase in bat sonar. *J. Acoust. Soc. Am.* **93**, 1553–1562 (1993).
26. S. Schmidt, B. Türke, B. Vogler, Behavioral audiogram from the bat, *Megaderma lyra*. *Myotis* **21–22**, 62–66 (1984).
27. R. B. Coles, A. Guppy, M. E. Anderson, P. Schlegel, Frequency sensitivity and directional hearing in the gleaning bat, *Plecotus auritus* (Linnaeus 1758). *J. Comp. Physiol. A* **165**, 269–280 (1989).
28. M. Konishi, How the owl tracks its prey. *Am. Sci.* **61**, 414–424 (1973).
29. W. D. Neff, J. E. Hind, Auditory thresholds of the cat. *J. Acoust. Soc. Am.* **27**, 480–483 (1955).
30. S. E. Currie, A. Boonman, S. Troxell, Y. Yovel, C. C. Voigt, Echolocation at high intensity imposes metabolic costs on flying bats. *Nat. Ecol. Evol.* **4**, 1174–1177 (2020).
31. D. J. Hartley, Stabilization of perceived echo amplitudes in echolocating bats. II. The acoustic behavior of the big brown bat, *Eptesicusfuscus*, when tracking moving prey. *J. Acoust. Soc. Am.* **91**, 1133–1149 (1992).
32. S. Hiryu, T. Hagino, H. Riquimaroux, Y. Watanabe, Echo-intensity compensation in echolocating bats (*Pipistrellus abramus*) during flight measured by a telemetry microphone. *J. Acoust. Soc. Am.* **121**, 1749–1757 (2007).
33. J. C. Koblitz, P. Stilz, W. Pflästerer, M. L. Melcón, H.-U. Schnitzler, Source level reduction and sonar beam aiming in landing big brown bats (*Eptesicus fuscus*). *J. Acoust. Soc. Am.* **130**, 3090–3099 (2011).
34. T. Budenz, A. Denzinger, H.-U. Schnitzler, Reduction of emission level in approach signals of greater mouse-eared bats (*Myotis myotis*): No evidence for a closed loop control system for intensity compensation. *PLOS ONE* **13**, e0194600 (2018).
35. L. Stidsholt, R. Müller, K. Beedholm, H. Ma, M. Johnson, P. T. Madsen, Energy compensation and received echo level dynamics in constant-frequency bats during active target approaches. *J. Exp. Biol.* **223**, jeb217109 (2020).
36. A. Denzinger, H.-U. Schnitzler, Echo SPL, training experience, and experimental procedure influence the ranging performance in the big brown bat, *Eptesicus fuscus*. *J. Comp. Physiol. A* **183**, 213–224 (1998).
37. K. R. Measor, B. C. Leavell, D. H. Brewton, J. Rumschlag, J. R. Barber, K. A. Razak, Matched behavioral and neural adaptations for low sound level echolocation in a gleaning bat, *Antrozous pallidus*. *eNeuro* **4**, ENEURO.0018-17 (2017).
38. S. Brinkløv, L. Jakobsen, J. M. Ratcliffe, E. K. V. Kalko, A. Surlykke, Echolocation call intensity and directionality in flying short-tailed fruit bats, *Carollia perspicillata* (*Phyllostomidae*). *J. Acoust. Soc. Am.* **129**, 427–435 (2011).
39. S. Brinkløv, E. K. V. Kalko, A. Surlykke, Dynamic adjustment of biosonar intensity to habitat clutter in the bat *Macrophyllum macrophyllum* (*Phyllostomidae*). *Behav. Ecol. Sociobiol.* **64**, 1867–1874 (2010).
40. M. Warnecke, W.-J. Lee, A. Krishnan, C. F. Moss, Dynamic echo information guides flight in the big brown bat. *Front. Behav. Neurosci.* **10**, 81 (2016).
41. K. Kugler, H. Luksch, H. Peremans, D. Vanderelst, L. Wiegrebe, U. Firzlaff, Optic and echo-acoustic flow interact in bats. *J. Exp. Biol.* **222**, jeb195404 (2019).
42. K. Egert-Berg, E. R. Hurme, S. Greif, A. Goldstein, L. Harten, L. G. Herrera, M. J. J. Flores-Martínez, A. T. Valdés, D. S. Johnston, O. Eitan, I. Borissov, J. R. Shipley, R. A. Medellin, G. S. Wilkinson, H. R. Goerlitz, Y. Yovel, Resource ephemerality drives social foraging in bats. *Curr. Biol.* **28**, 3667–3673.e5 (2018).
43. R. P. Wilson, M. P. Wilson, Dead Reckoning: A new technique for determining penguin movements at sea. *Meeresforschung.* **32**, 155–158 (1988).
44. R. P. Wilson, N. Liebsch, I. M. Davies, F. Quintana, H. Weimerskirch, S. Storch, K. Lucke, U. Siebert, S. Zankl, G. Müller, I. Zimmer, A. Scolaro, C. Campagna, J. Plötz, H. Bornemann, J. Teilmann, C. R. McMahon, All at sea with animal tracks; methodological and analytical solutions for the resolution of movement. *Deep Sea Res. II Top. Stud. Oceanogr.* **54**, 193–210 (2007).
45. R. J. Urick, *Principles of Underwater Sound* (Peninsula Pub, ed. 3, 1983).

46. K. Ghose, C. F. Moss, Steering by hearing: A bat's acoustic gaze is linked to its flight motor output by a delayed, adaptive linear law. *J. Neurosci.* **26**, 1704–1710 (2006).

**Acknowledgments:** We thank A. Hubancheva for discussions and J. Goldbogen and C. Elemans for comments on the earlier version of the manuscript. **Funding:** This study was funded by the Carlsberg Semper Ardens grant to P.T.M. and by the Emmy Noether program of the Deutsche Forschungsgemeinschaft (DFG; German Research Foundation, grant no. 241711556) to H.R.G. All experiments were carried out under the following licenses: 721/12.06.2017, 180/07.08.2018, and 795/17.05.2019. **Author contributions:** L.S. was responsible for data collection, programming, analysis, interpretation, and drafting of the manuscript. S.G. was responsible for conceptualization, data collection, and interpretation of the data. H.R.G. interpreted the data. K.B. programmed and analyzed the data. J.M. programmed software for data analysis. M.J. designed and manufactured the tags and contributed to the analysis and interpretation of the data. P.T.M. designed the experiment, analyzed, and interpreted the data. All authors contributed to the writing of the manuscript. **Competing interests:** The authors declare that they have no competing interests. **Data and materials availability:** All data needed to evaluate the conclusions in the paper are present in the paper and/or the Supplementary Materials. Additional data related to this paper may be requested from the authors.

Submitted 6 October 2020
Accepted 21 January 2021
Published 3 March 2021
10.1126/sciadv.abf1367

**Citation:** L. Stidsholt, S. Greif, H. R. Goerlitz, K. Beedholm, J. Macaulay, M. Johnson, P. T. Madsen, Hunting bats adjust their echolocation to receive weak prey echoes for clutter reduction. *Sci. Adv.* **7**, eabf1367 (2021).

# Hunting bats adjust their echolocation to receive weak prey echoes for clutter reduction

Laura Stidsholt, Stefan Greif, Holger R. Goerlitz, Kristian Beedholm, Jamie Macaulay, Mark Johnson and Peter Teglberg Madsen

*Sci Adv* **7** (10), eabf1367.
DOI: 10.1126/sciadv.abf1367

Science Advances
AAAS

advances.sciencemag.org/cgi/content/full/7/10/eabf1367/DC1

# Supplementary Materials for

## Hunting bats adjust their echolocation to receive weak prey echoes for clutter reduction

Laura Stidsholt*, Stefan Greif, Holger R. Goerlitz, Kristian Beedholm, Jamie Macaulay, Mark Johnson, Peter Teglberg Madsen

*Corresponding author. Email: laura.stidsholt@bio.au.dk

Published 3 March 2021, *Sci. Adv.* **7**, eabf1367 (2021)
DOI: 10.1126/sciadv.abf1367

**The PDF file includes:**



**Other Supplementary Material for this manuscript includes the following:**

(available at advances.sciencemag.org/cgi/content/full/7/10/eabf1367/DC1)

**Supplementary Text**

In this supplementary section, we present extended data from the tagging study in the field, but also from two different experiments in flight rooms to validate and ground truth the data from the wild. We have structured the supplementary text by first presenting the data from the tagging study (1) and then the calibration and validation experiments in the laboratory (2). The final section is a detailed description of how sensory volumes and redundancies were calculated (3).

1. Field study:

The weights and sizes of the tagged bats and the on-board tags are summarised in Table S1. The foraging attempts for all bats are summarised in Table S2. To extract the echo streams from clutter and prey, we tracked echo streams on all echograms of the aerial captures. The beginning and end of the prey echo streams were manually marked. The approach speed was indicated by the slope of the echo streams (Figure S1). Clutter streams were tracked on all echograms of foraging attempts. Clutter was present in the auditory scenes of all bats (Figure S2). As the bats decreased their output levels towards prey capture, the prey and clutter echo levels develop differently due to the different transmission losses between the prey at close ranges and clutter structures at longer distances. This is modelled for an insect with a target size of -30 dB with clutter present two meters behind the insect (Figure S6).

2. Calibration and validation experiments in a flight room:

We used seven Greater mouse-eared bats caught at Orlova Chuka cave in Rusenski Lom Nature Park, Northeastern Bulgaria, for our laboratory studies. The bats were kept at the Siemers Bat Research Station between experiments. The tags weighed 2.6 grams in the laboratory studies.
The validation experiments in the flight room consisted of two studies:

(1) A target approach experiment in a laboratory, where tagged bats were flying towards a target sphere with an array behind to quantify the relationship between the sound recorded on the tag and the sound that is emitted by the bat into the forward direction.

(2) A prey capture experiment, where tagged bats were trained to catch tethered moths to ground-truth the data recorded by the tag when bats are catching aerial prey.

2.1. Target approach experiment for SL estimations

We trained two female Greater mouse-eared bats (body weight: ~27 g) to fly across a flight room (4 x 8 m, 2.3 m high) and to land on a target sphere (diameter: 20 cm) while carrying the tag. An eight-microphone (Knowles, FG23329) recording array was covered in acoustic foam and placed behind the target to record all emitted echolocation calls. The array microphones were pre-amplified by a custom-made amplifier (40 dB) and recorded with a sampling rate of 250 kHz, a clipping level of 106 dBre20µPa and a 1-pole, 10 kHz analog high-pass filter. When the bats landed on the target, a speaker behind the target emitted a unique synchronization sound (1 to 8 kHz, 5 ms). The synchronization sound served to synchronize the tag and array data as well as indicate a successful trial to the bat. The bats were then fed a mealworm. As the tag (2.6 g) weighed 10 % of the body mass of the bats, we carefully monitored the bats during the experiments for any

sign of discomfort or fatigue, but found none. We conducted 51 trials (28 and 23 for each bat respectively) lasting approximately 30 minutes per bat.
Tag and array audio data were adjusted for the frequency response of the respective recording system (*10*) and high-pass filtered by a 4-pole 10 kHz high pass Butterworth filter to extract only the echolocation calls. Accelerometer data were low-pass filtered with a delay-free linear phase finite impulse response (FIR) filter with a cut-off frequency of 30 Hz. All analyses were conducted using custom-written scripts (Matlab, 2019a, The Mathworks, Natick, MA, USA).
As the calls of the bats were emitted in a directional beam in front of the bat, we conducted the target approach experiment to calculate the difference in call levels between on-axis calls recorded by the array (SL) and the off-axis calls recorded by the tag (Apparent output levels, AOL).
The tag and array data were synchronized by cross-correlation with the unique synchronization sound. SLs were calculated from the received levels recorded by the array (sensu(*35*)). The energy flux density (EFD) of the calls were extracted over a -6 dB energy window both on the array and on the tag. The average difference between AOLs and SLs was ~4 dB (Figure S4). This offset was used to estimate SL directly from the wild tag recordings.

2.2. Prey capture

To be able to recognize and understand the field data during aerial captures, we conducted prey capture experiments with five trained *Myotis myotis* bats in the same flight room as above. The bats flew individually in the flight room and attacked tethered mealworms or moths in different sizes and from different families while carrying the tag. The bats caught 15 moths each in approximately one hour of instrumentation with the tag. All buzzes emitted when the bats where flying and catching moths were associated with a prey capture attempt. Loud chewing sounds audible in the tag recordings just after prey capture indicated a successful capture.
To groundtruth potential aerial prey captures in the field, we analyzed the audio data of aerial prey captures in the flight room. We estimated SLs in EFD by adding 14 dB to the AOLs recorded on the tag over a -6 dB energy window. To extract prey echoes from each call, we visualized the acoustic streams of each capture in echograms (Figure S2) (*10*). The closing echo stream of the prey was clearly visible (Figure S5) just prior to prey capture. Prey echoes were identified as a sequence of short echoes returning at gradually shorter time-intervals prior to a buzz (Figure S2C). In the buzz, it was usually not possible to extract echoes. To extract the range of the returning prey echoes and the echo level (Figure S5A) from each emitted call during a capture, we tracked the closing echo stream of prey on the echograms (Figure S5C). The prey echoes were weak due to a combination of small targets, weaker SLs used in the flight room compared to in the wild, strong clutter echoes from the echoic flight room, as well as the small size of the flight room leaving a small perceptual overlap free zone. Thus, it was difficult to automatically extract echoes. Instead, we manually marked the beginning and end of the stream (Figure S5A, white dashed line). The regression line between these two points were then used as a window to look for echo peaks in the cross correlation between the call and the time interval to the next call (each vertical bar on the echogram). For each vertical bar in the echogram, the position and the peak of the echo level in the corresponding window was extracted (Figure S6).

The peak of the cross correlation at the position of the echo could be converted into echo level in EFD by dividing the peak with the energy of the call template:

$$Peak\ of\ cross\ correlation\ at\ echo\ position = E(call) * E(echo) \qquad (1)$$

$$E(echo) = 20 * log10\left(\frac{peak\ of\ xcorr}{\left(\sqrt{sum(call^2)}\right)}\right) - 10 * log10(sampling\ rate)$$

The lowest extracted echoes levels were ~5 dB re 20 µPa$^2$s. The tag can record these echo levels due to the high processing gain of the calls of up to 22 dB ($10 * \log10((80\ \text{kHz} - 24\ \text{kHz}) * 0.003\ \text{sec})$ = 22 dB). By using SL, EL and range to the insect, R, we calculated the target strengths (TS) of the moths by using the sonar equation (*45*). During a capture, TS was calculated between one to many times depending on how many echoes it was possible to extract from the echograms.

3. Sensory volumes and redundancy:

To calculate the beam shape and size, we constructed a 3D mesh around the position of the bat (Figure S7, all dots). We calculated the sensory volumes (SV) by finding all the points in the 3D grid where the bat could detect its prey by the given SL of the call using this equation:

$$SV = RL(x) > RLT \qquad (2)$$

RL(x) is the received level at each grid point (x) based on the SL of the bat, the transmission loss and target strength of the prey

RLT is the received level threshold, which is used as a threshold to determine which 3D grid points (x) is included in the sensory volume (SV).

SV is the volume surrounding the cloud of grid points above the RLT

To estimate the RLT, we calculated the maximum range ($R_{max}$) at which the bat could detect the prey using the SL, TS and sonar equation. The RLT is then calculated as:

$$RLT = SL - 20 * log10\left(\frac{R_{max}}{0.1m}\right) + TS \qquad (3),$$

Next, we found the RL at each grid point to be able to use equation 2 to find the grid points with RL above the threshold. For each grid point (x) in the mesh (Figure S7, dots), we calculated the received level (RL) based on the distance to the grid point and the off-axis angle determining the beam loss at that specific position according to the piston model:

$$RL\ (x) = SL - TL(x) + TS - BL(x) \qquad (4),$$

where RL is the received level at the grid point x, SL is the source level measured on the tag, and TS is the target size. TL is the one-way transmission loss based on the distance between the bat and the grid point x, and BL is the beam loss at the grid point x based on the filtering properties of the piston-model.

The beam loss (BL) is calculated using the piston-model. Here, we calculated the beam loss at each angle ($\theta$) off the beam direction axis for both a search (blue) and a buzz (red) call (Figure S8). The beam direction was defined in the direction of a vector (v) following the dead-reckoning track 200 ms after the sound emission of the bat based on a study showing that the flight path was following the beam direction with a delay of 140 to 230 ms (*46*).

To calculate the BL per grid point (x), the distance (d) and the off-axis-angle ($\theta$) between the direction of the flight path and the grid point was calculated.

Distance (d): For each grid point in the 3D mesh, a vector from the position of the bat to the grid point was found (u) (Figure S7). The length of this vector is the distance to the grid point. This distance is used to calculate TL in equation 4.
Off-axis-angle ($\theta$): A vector pointing in the beam direction (v) following the flight path was defined. We found the angle between the vectors v and u for all grid points in the mesh by the cross product:

$$\theta = cos(dot(v,u)) \qquad (5),$$

The beam loss at the grid point can be found for each angle ($\theta$) (Figure S8) which is used in equation 4 to estimate RL at the position x.
Thus, each grid point (x) in space has a specific RL. All grid points with RLs above the RLT (green, purple dots Figure S7) are extracted (based on equation 2). The volume including all these points constitutes the sensory volume in 3D (Figure S7, blue and grey patches).

The resolution of the sensory volumes depends on the grid size (GS) (*i.e.* distance (m) between grid points in the 3D mesh). As the SLs varied dramatically over the entire capture, GS was matched to the SLs to avoid too long computational times. Sensory volumes estimates for different SLs (40, 60, 80, and 100 dB re 20µPa$^2$s) were plotted against different values of GS (Figure S9A). The GS leading to an error below 15 % was chosen for each of the SLs (Figure S9A, black dots). An exponential equation was fitted to the data to estimate the suitable GS for each SL varying from 20 to 120 dB re 20µPa$^2$s SLs (Figure S9B):

$$GS = 0.0015 * e^{SL*0.0486}$$

The GS of mirror targets (for the commuting flights) were 8 times larger.

3.1 Calculations of redundancy:
For each aerial capture, the data was divided into search, approach and buzz phase (see above). The sensory volumes of all calls in the three phases were calculated in the same large 3D mesh (Figure S7). To calculate the redundancy (*i.e.* the number of times the same volume of air was ensonified) for each of the three categories, we used the ratio between the sums of all individual sensory volumes in each category (Figure S10, above black lines top) divided by the sum of the overall surface of all sensory volumes (Figure S10, grey grid).

$$Redundancy(y) = \frac{\sum_{i=1}^{N} V(SV)}{V(overall\ 3D\ shape)} \qquad (5)$$

y = foraging phase (search, approach or buzz phase)
N = number of calls in each phase,
V = volume of either each call or the overall shape
SV = sensory volumes per call

**Figure S1.**

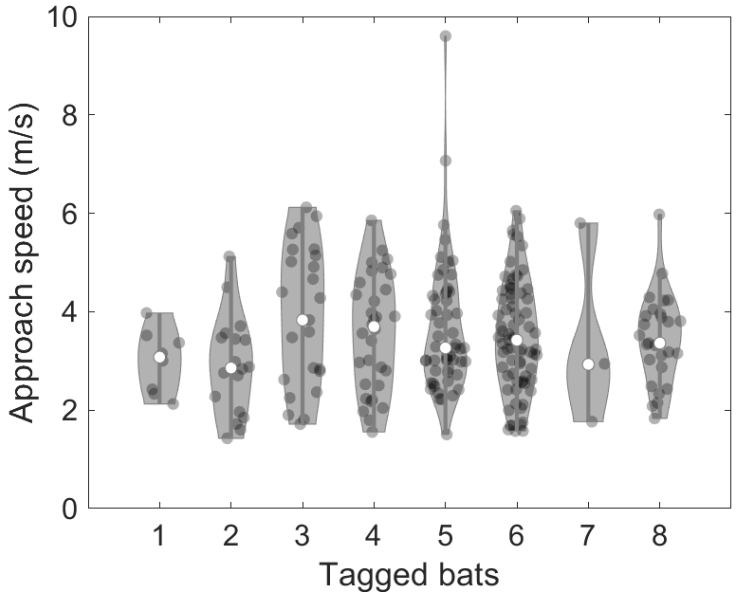


**Approach speed between the bat and its prey.** The slope of the linear regression line based on the best fit of the tracked prey echoes streams on the echograms corresponded to the speed at which the bat homed in on its prey. Across all individuals and captures, the approach speeds ranged from 1.5 to 6 m/s (N = 8 bats and 246 captures).

**Figure S2.**

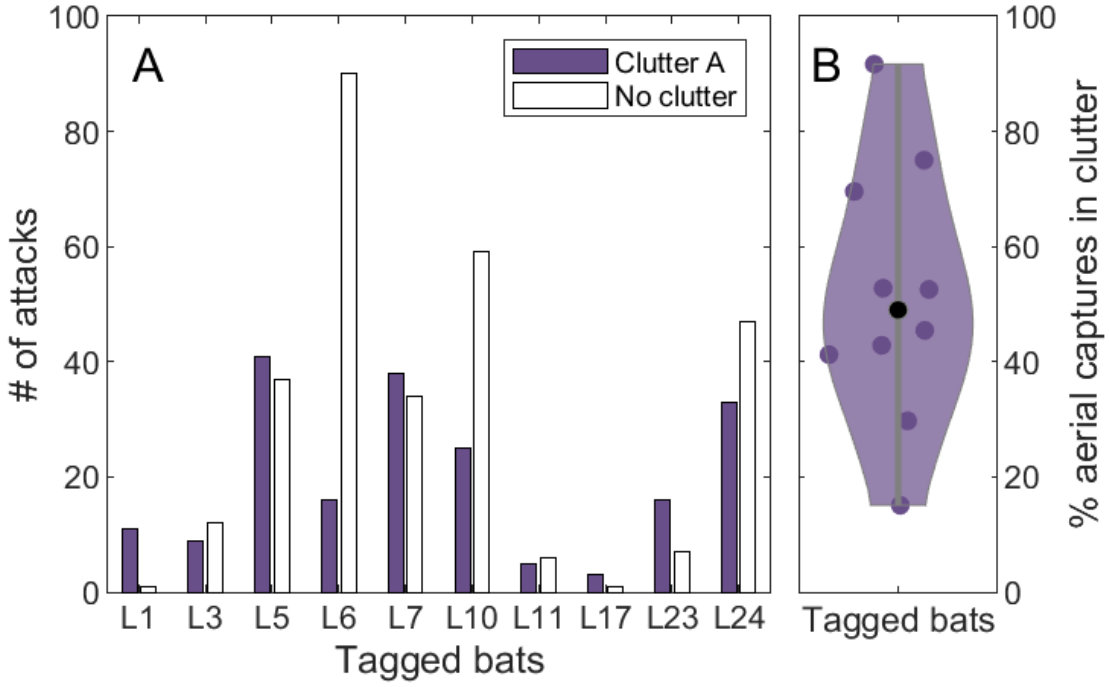


**Clutter distribution during aerial captures.** a, Distribution of whether clutter was present or not during the last three seconds before prey capture for all individually tagged bats. b, Clutter was present in around half of the captures; dots show percentages for each bat individual. Total N = 457 captures, where 260 were in clutter.

**Figure S3.**

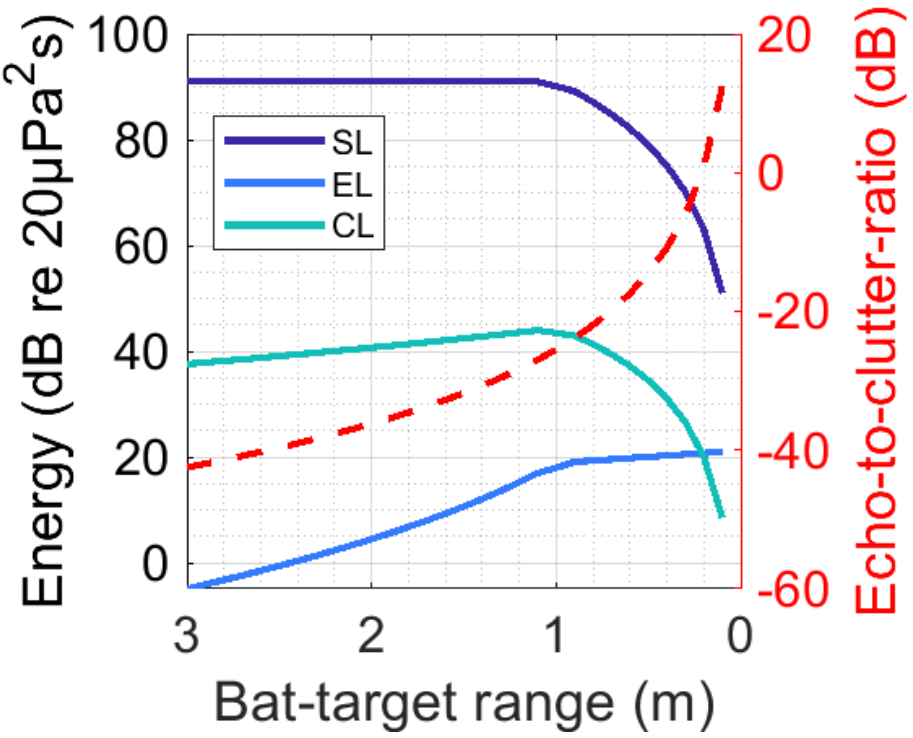


**Development in echo and clutter levels when bats adjust their source levels to target range**. This theoretical bat emits calls with constant output levels (dark blue) until about one meter from the prey, where the bat then adjusts its SLs by $29\text{Log}_{10}$(target range). The returning prey echo levels (TS = -30 dB, point-target) increase until a certain threshold, where they level off (light blue). Clutter (TS = -10 dB, mirror-target) is in this calculation located two meters behind the prey. Clutter levels (green) therefore increase less dramatically in comparison to ELs, which results in an increase in the echo-to-clutter-ratio (red) throughout the capture (red).

**Figure S4.**

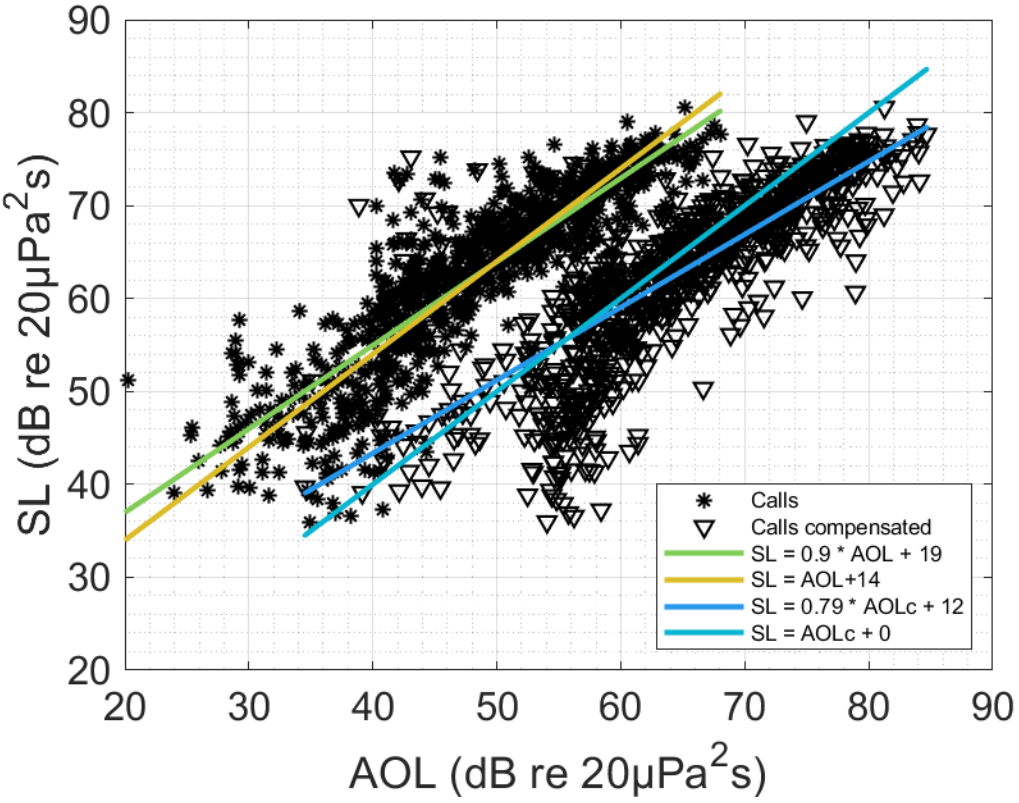


**Estimating call source levels (SL) from tag-recorded apparent output levels (AOLs) in a target approach experiment.** SLs were extracted from on-axis recordings on the array and plotted against the AOLs (stars) extracted from the tag recordings. By applying the back-to-front transfer function to AOLs, the compensated calls were similar to SLs (triangles). The slopes of the linear regression lines for AOL vs SLs (green) and AOLc vs SL (dark blue) were different from 1. By forcing the linear fit to have a slope of 1 (yellow and light blue), we can estimate the average offset between the sound recorded on the tag and the sound as emitted by the bat into the forward direction. The average offset iS14 dB (difference between the yellow and light blue regression lines). N = 1443 calls.

**Figure S5.**

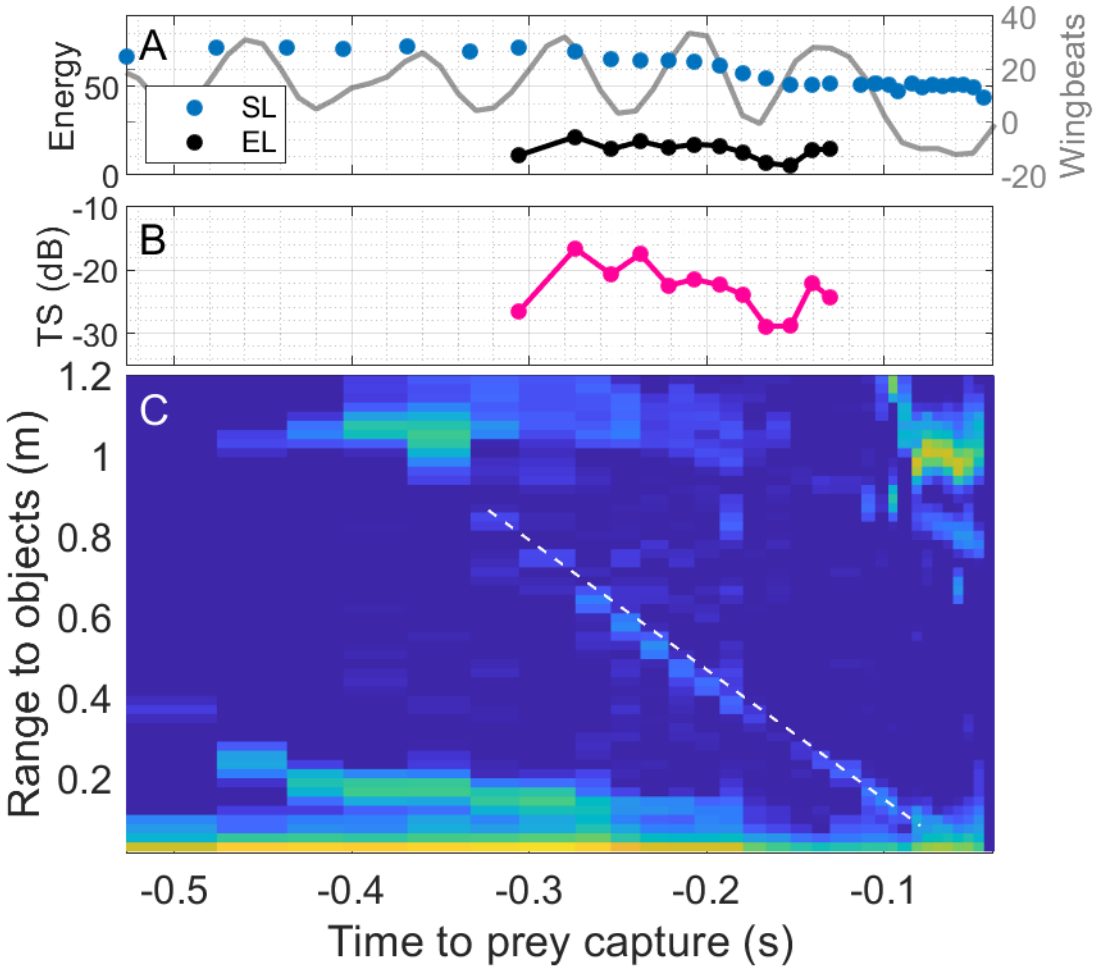


**Synchronized biosonar output adjustments, returning sensory scene and movement over the course of a successful capture of a tethered large moth.** The source levels (SL, blue) and echo levels (EL, black) over the time to prey capture (A) was used to calculate the target strength (TS) of the insect (B). The maximum TS was -16 dB. The prey echo stream was clearly visible in the echogram the last 0.3 seconds and 0.9 meters of the capture (C). Notice, clutter from the flight room at above one meters distance.

**Figure S6.**

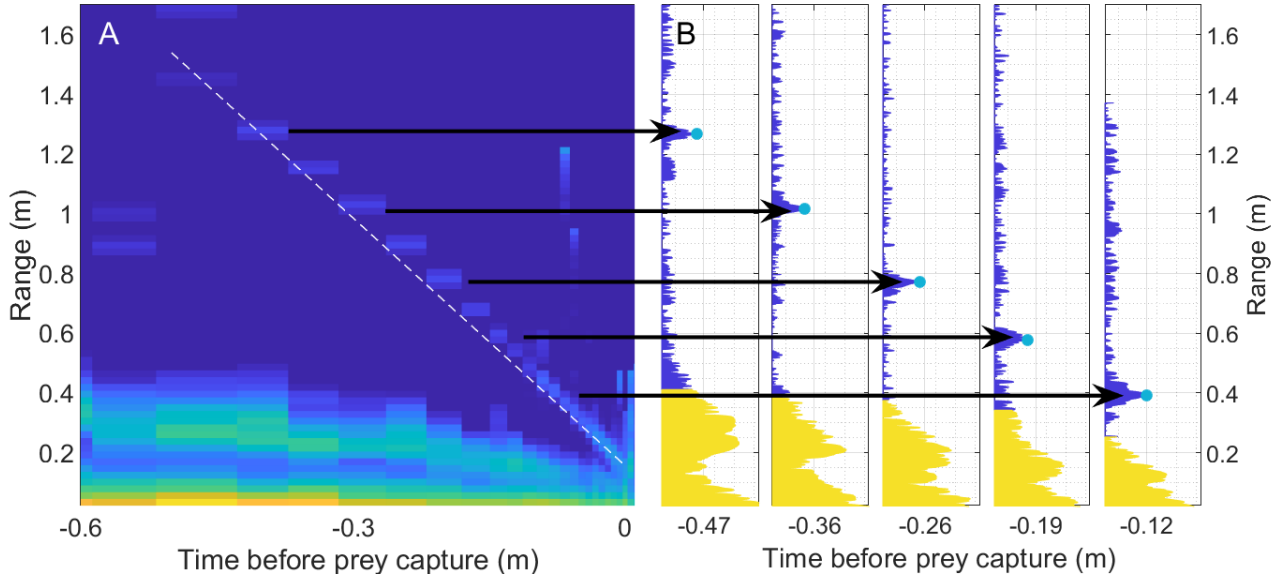


**Visualization of the echogram-tracking of prey streams. a**, The echogram consists of vertical bars aligned horizontally after each other. Each vertical bar is a cross-correlation of the outgoing call with the audio data until the next call emission. To guide the extraction of the correct echoes, we manually tracked the prey echo stream on each echogram. The regression line was calculated (dashed white line) and used to find a proper window of the cross-correlation of each call-echo pair. **b**, An example of the cross-correlation of five different call-echo streams from the approach. Calls are colored yellow, echo stream colored blue. The same echoes were visible both in the echogram (**a**) and marked as peaks of the cross-correlation (blue dots) in a +/- 0.5 ms window around the regression line (black arrows).

**Figure S7.**

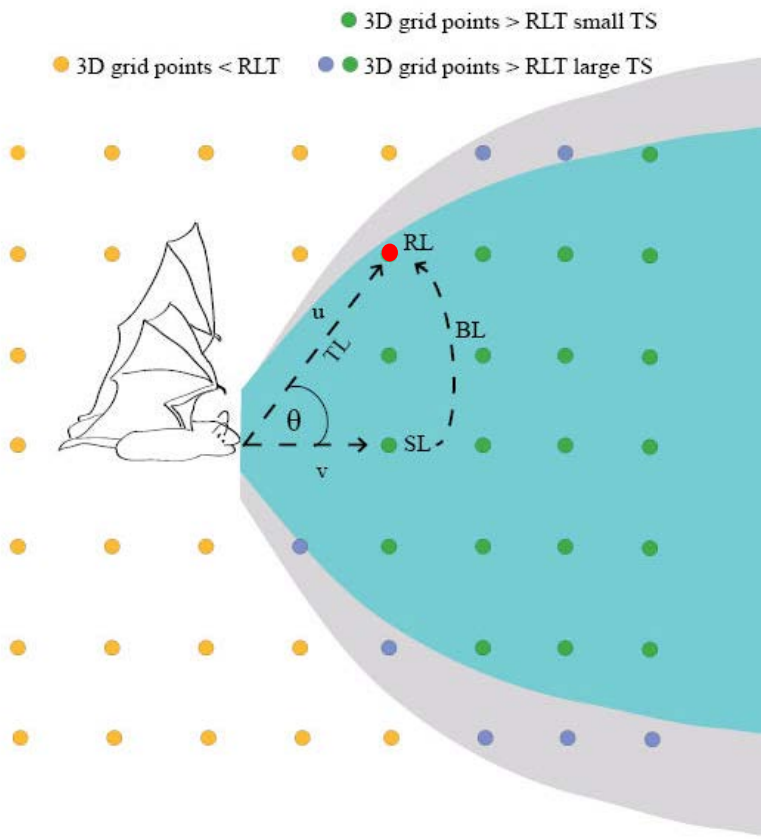


**Visualization of the framework to find the sensory volumes.** The bat is emitting a call and ensonifying a sensory volume in front of itself. We have calculated the RL at each point in the grid around the bat (dots) based on equation 2. To calculate the RL, two vectors are defined: A vector (v) following the flightpath of the bat and a vector (u) from the position of the bat to the grid point of interest (x, red dot). The angle ($\theta$) between the two vectors is used to estimate the beam loss (BL) and the length of vector u (=distance between bat and x) is used to calculate the transmission loss (TL). The sensory volume (blue and grey patches) is then defined as the volume of the points above the received level threshold (RLT). The RLT vary according to target size. For a large TS, the sensory volume is large (grey patch including both green and blue dots). For a small TS, the sensory volume is smaller (blue patch, only green dots).

**Figure S8.**

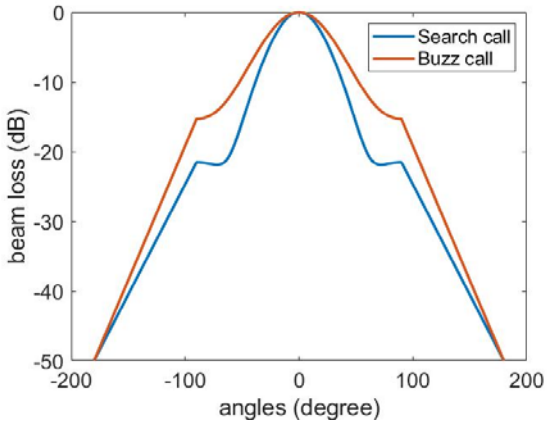


**Beam loss for each off-axis angle based on the filtering properties of the piston-model.** As the piston-model assumes a symmetrical beam, the beam loss curves are rotational-symmetric around the main axis. The beam loss is smaller for the buzz at each off-axis angle (red), as it has a lower frequency content and thus a lower directionality. The buzz beam loss was used in the calculations for all calls emitted with an intercall interval below 10 msec.

**Figure S9.**

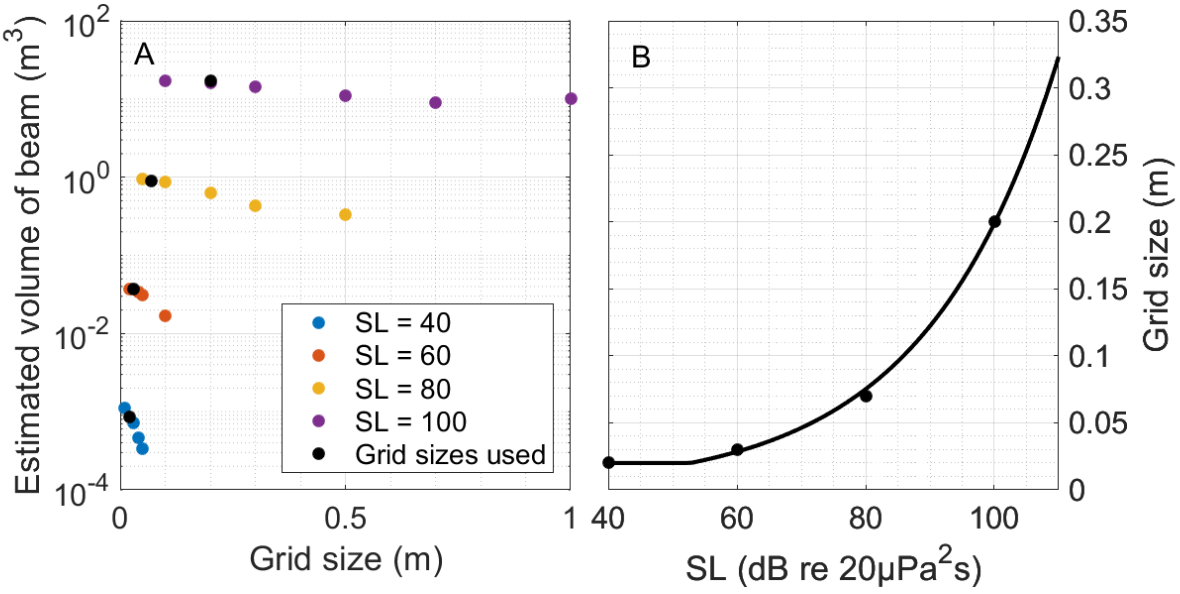


**Grid resolution and sensory volume-estimates for different SL values. a,** The sensory volume-estimates for each SL (colors) were based on different grid size (GS). The smaller the grid size, the better an estimate of the sensory volumes as the resolution of the 3D shapes improve. The grid sizes used to fit the relationship between SL and GS in panel **b** were chosen to avoid too long computational times but at the same time to still maintain an estimate for the sensory volumes with an error of 5-15 %.
**b**, The grid sizes used per SL from A (black dots) were fitted to an exponential function (black solid line) and used to find GS for each SL in the recordings.

**Figure S10.**

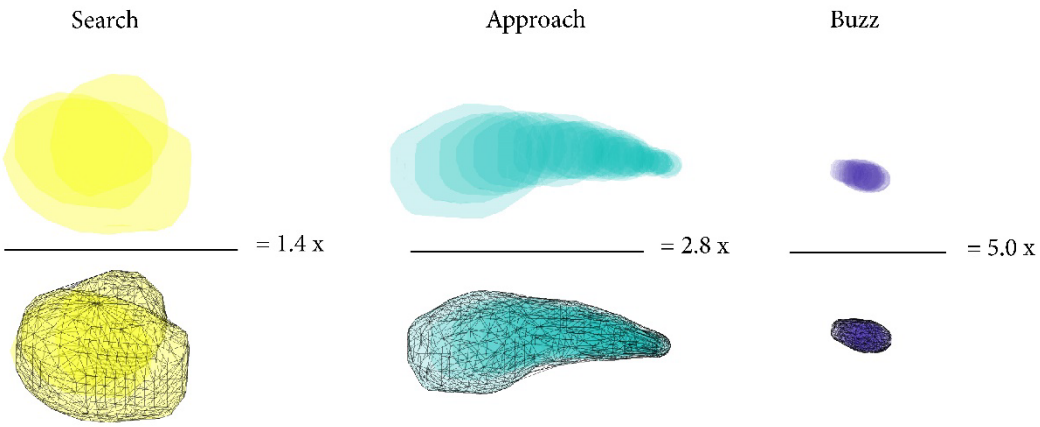


**Example of calculations of redundancies for each phase.** The sum of the individual volumes (above the black line) is divided by the volume within the overall mesh (grey grid) around the individual beams in each phase (search, approach and buzz).

**Table S1.**

| Bat ID | Year | Sex & status | Weight at capture | Weight at release | Diurnal weight loss | Bat weight recapture | Tagging weight loss | Tag weight | Tag weight % | CM3 (mm) | Forearm length (mm) |
|---|---|---|---|---|---|---|---|---|---|---|---|
| L17 | 2017 | f, PL | - | 30 | - | 27.3 | 2.7 | 3.5 | 11.7 | - | - |
| L1 | 2018 | f, L | 37.9 | 31.2 | 6.7 | 29.5 | 1.7 | 4 | 12.8 | - | - |
| L3 | 2018 | f, L | 36 | 30.1 | 5.9 | 27.3 | 2.8 | 3.7 | 12.3 | - | - |
| L5 | 2018 | f, L | 35.8 | 30.5 | 5.3 | 28 | 2.5 | 4 | 13.1 | 10 | 66.7 |
| L6 | 2018 | f, L | 36.2 | 29.8 | 6.4 | 27.1 | 2.7 | 3.8 | 12.8 | 9.8 | 64.1 |
| L7 | 2018 | f, L | 34.8 | 29.4 | 5.4 | 25.1 | 4.3 | 3.6 | 12.2 | 10 | 64 |
| L10 | 2018 | f, L | 36.1 | 30.1 | 6 | 27.1 | 3 | 3.5 | 11.6 | 10 | 66.1 |
| L11 | 2018 | f, PL | 33.1 | 29.3 | 3.8 | - | - | 4 | 13.7 | 10.1 | 66.1 |
| L23 | 2019 | f, PL | 33.2 | 28 | 5.2 | 27.1 | 0.9 | 3.5 | 12.5 | 10 | 63.4 |
| L24 | 2019 | f, PL | 33.6 | 28.9 | 4.7 | - | - | 3.8 | 13.1 | - | - |

**Summary of the weights and sizes of the tagged bats.** All weights are in grams. f: female, PL: post-lactating, L: lactating. If recapture weights of the bats is missing, the tags were found on the ground below the colony.

**Table S2.**

| Bat ID | Total aerial attacks | Successful aerial attacks | Proportion of aerial attacks with clutter (%) | Total ground attacks |
|---|---|---|---|---|
| L1 | 12 | 11 | 92 | 59 |
| L3 | 21 | 18 | 43 | 68 |
| L5 | 77 | 62 | 58 | 11 |
| L6 | 103 | 75 | 13 | 0 |
| L7 | 71 | 55 | 50 | 5 |
| L10 | 82 | 65 | 30 | 3 |
| L11 | 11 | 11 | 45 | 179 |
| L17 | 4 | 4 | 25 | 33 |
| L23 | 23 | 19 | 70 | 166 |
| L24 | 79 | 62 | 43 | 56 |
| **Mean** | **48** | **38** | **47** | **58** |

**Summary of the foraging attempts and captures of ten *Myotis myotis*.** The bats attempted to catch both aerial prey (total aerial attacks) and ground-based prey (total ground attacks). The successful aerial prey captures were validated by chewing sounds just after the buzz (SuppleVideo 1). The bats were often foraging close to vegetation, which is indicated by the percent of the total aerial attacks where clutter was present.

**Table S3**

**Generalized linear mixed-effect model analysis for the relationship between the presence of clutter and the acoustic and movement behavior.** Presence or absence of clutter (clutter) was the response variable (binomial distribution with "cauchit" link). The fixed-effect variables were output adjustments across six successive calls and the maximum changes in flight path presumable before prey detection (2 seconds before prey capture) ($SL_{2sec}$ and $MA_{2sec}$) Each individual bat was added as random effect (AnimalNo). The hypothesis was tested via the model: Clutter ~ $SL_{2sec}$+$MA_{2sec}$+(1|AnimalNo). Exp. deviance in the table is how much deviance each predictor variable explains.

| Name in model | Predictor variable | Effects (SD) | pvalue | Exp. deviance |
|---|---|---|---|---|
| $SL_{2sec}$ | Slope of the six nearest call source levels (SL change/10 ms) | -0.027 (0.01) | 6.5e-5 | 43% |
| $MA_{2sec}$ | Maximum change in flight path during the six nearest calls (degree) | 1.480 (0.27) | 7.9e-8 | 57% |

**Movie S1.**

**Flight path and beam of echolocation calls during aerial capture**. The flight path and the sensory volumes (coloured shapes) show how the bat manoeuvers in 3D and adjusts its sensory volumes to capture a flying insect. The search (yellow), approach (light blue) and buzz (dark blue) phases are easy to identify. The movement of the insect (black drawing) is unknown and therefore depicted randomly.

**Movie S2.**

**Sensory scene, vocal outputs and movement of a bat hunting several insects.** The returning sensory scene from the environment is visualized in an echogram (upper panel). The vocal outputs are depicted as colored dots (middle panel) and show how the bats change their output levels and repetition rate (colors) when they interact with their environment. The wingbeats (blue) and orientation (red) (lower panel) changes during the pursuit of prey and are correlated with changes in the vocal outputs. The bat is intercepting seven prey items (moth drawing) and only successfully capture the last insect (green circle) indicated by chewing sounds at the end of the movie. The bat is approaching large background structures as trees (tree drawings) when they are hunting.

**Audio S1.**

**On-board sound clip of a bat capturing an insect on the wing**. The bat is searching, approach and capturing prey (at 5 seconds into the file) while emitting echolocation calls that are audible at high frequency. The bat continues its flight path for ten seconds before it starts to chew its prey (at 17 seconds into the file). The chewing sounds are lower in frequency and can be heard between individual echolocation calls. The audio signal has been high-pass filtered at 100 Hz to exclude wind-noise from wingbeats.

**Audio S2.**

**On-board sound clip of a bat chewing while flying**. The chewing is fast because the bat chews between emission of echolocation calls. The calls are timed to the wingbeats and therefore the bats is chewing seven times per second in this clip. The audio signal has been band-pass filtered (0.25 to 18 kHz) to exclude wind-noise from wingbeats and echolocation calls.

## REFERENCES AND NOTES


1. M. S. Lewicki, B. Olshausen, A. Surlykke, C. F. Moss, Scene analysis in the natural environment. *Front. Psychol.* **5**, 199 (2014).

2. D. R. Griffin, Echolocation by blind men, bats and radar. *Science* **100**, 589–90 (1944).

3. A. Surlykke, C. F. Moss, Echolocation behavior of big brown bats, *Eptesicus fuscus*, in the field and the laboratory. *J. Acoust. Soc. Am.* **108**, 2419–29 (2000).

4. L. Jakobsen, M. N. Olsen, A. Surlykke, Dynamics of the echolocation beam during prey pursuit in aerial hawking bats. *Proc. Natl. Acad. Sci. U.S.A.* **112**, 8119–8123 (2015).

5. D. R. Griffin, F. A. Webster, C. R. Michael, The echolocation of flying insects by bats. *Anim. Behav.* **8**, 141–154 (1960).

6. D. A. Cahlander, J. J. G. Mccue, F. A. Webster, The determination of distance by echolocating bats. *Nature* **201**, 544–546 (1964).

7. E. K. V. Kalko, Insect pursuit, prey capture and echolocation in pipestirelle bats (*Microchiroptera*). *Anim. Behav.* **50**, 861–880 (1995).

8. M. W. Holderied, C. Korine, M. B. Fenton, S. Parsons, S. Robson, G. Jones, Echolocation call intensity in the aerial hawking bat *Eptesicus bottae* (*Vespertilionidae*) studied using stereo videogrammetry. *J. Exp. Biol.* **208**, 1321–1327 (2005).

9. A. R. Wheeler, K. A. Fulton, J. E. Gaudette, R. A. Simmons, I. Matsuo, J. A. Simmons, Echolocating big brown bats, *Eptesicus fuscus*, modulate pulse intervals to overcome range ambiguity in cluttered surroundings. *Front. Behav. Neurosci.* **10**, 125 (2016).

10. B. Mao, M. Aytekin, G. S. Wilkinson, C. F. Moss, Big brown bats (*Eptesicus fuscus*) reveal diverse strategies for sonar target tracking in clutter. *J. Acoust. Soc. Am.* **140**, 1839–1849 (2016).

11. B. Falk, L. Jakobsen, A. Surlykke, C. F. Moss, Bats coordinate sonar and flight behavior as they forage in open and cluttered environments. *J. Exp. Biol.* **217**, 4356–4364 (2014).

12. M. Taub, Y. Yovel, Segregating signal from noise through movement in echolocating bats. *Sci. Rep.*. **10**, 382 (2020)

13. L. Stidsholt, M. P. Johnson, K. Beedholm, L. Jakobsen, K. Kugler, S. Brinkløv, A. Salles, C. F. Moss, P. T. Madsen, A 2.6-g sound and movement tag for studying the acoustic scene and kinematics of echolocating bats. *Methods Ecol. Evol.* **10**, 48–58 (2019)

14. J. B. Snyder, M. E. Nelson, J. W. Burdick, M. A. MacIver, Omnidirectional sensory and motor volumes in electric fish. *PLOS Biol.* **5**, e301 (2007).

15. L. P. Tyrrell, E. Fernández-Juricic, The hawk-eyed songbird: Retinal morphology, eye shape, and visual fields of an aerial insectivore. *Am. Nat.* **189**, 709–717 (2017).

16. J. E. Boström, M. Dimitrova, C. Canton, O. Håstad, A. Qvarnström, A. Ödeen, Ultra-Rapid vision in birds. *PLOS ONE* **11**, e0151099 (2016).

17. C. Geberl, S. Brinkløv, L. Wiegrebe, A. Surlykke, Fast sensory–motor reactions in echolocating bats to sudden changes during the final buzz and prey intercept. *Proc. Natl. Acad. Sci.* **112**, 4122–4127 (2015).

18. D. M. M. Wisniewska, M. Johnson, J. Teilmann, L. Rojano-Doñate, J. Shearer, S. Sveegaard, L. A. A. Miller, U. Siebert, P. T. Madsen, Ultra-high foraging rates of harbor porpoises make them vulnerable to anthropogenic disturbance. *Curr. Biol.* **26**, 1441–1446 (2016).

19. J. Demšar, C. K. Hemelrijk, H. Hildenbrandt, I. L. Bajec, Simulating predator attacks on schools: Evolving composite tactics. *Ecol. Model.* **304**, 22–33 (2015).

20. T. Hügel, H. R. Goerlitz, Species-specific strategies increase unpredictability of escape flight in eared moths. *Funct. Ecol.* **33**, 1674–1683 (2019).

21. C. F. Moss, A. Surlykke, Auditory scene analysis by echolocation in bats. *J. Acoust. Soc. Am.* **110**, 2207–2226 (2001)

22. W. W. Wilson, C. F. Moss, Sensory-motor behavior of free-flying FM bats during target capture, in

*Echolocation in Bats and Dolphins*, J. A. Thomas, C. F. Moss, M. Vater, Eds. (The University of Chicago Press, 2004), pp. 22–27.

23. E. K. V. Kalko, H.-U. Schnitzler, Plasticity in echolocation signals of European pipistrelle bats in search flight: Implications for habitat use and prey detection. *Behav. Ecol. Sociobiol.* **33**, 415–428 (1993).

24. S. A. Kick, Target-detection by the echolocating bat, *Eptesicus fuscus*. *J. Comp. Physiol.* **145**, 431–435 (1982).

25. C. F. Moss, J. A. Simmons, Acoustic image representation of a point target in the bat *Eptesicus fuscus*: Evidence for sensitivity to echo phase in bat sonar. *J. Acoust. Soc. Am.* **93**, 1553–1562 (1993).

26. S. Schmidt, B. Türke, B. Vogler, Behavioral audiogram from the bat, *Megaderma lyra Myotis* **21–22**, 62–66 (1984).

27. R. B. Coles, A. Guppy, M. E. Anderson, P. Schlegel, Frequency sensitivity and directional hearing in the gleaning bat, *Plecotus auritus* (Linnaeus 1758). *J. Comp. Physiol. A* **165**, 269–280 (1989).

28. M. Konishi, How the owl tracks its prey. *Am. Sci.* **61**, 414–424 (1973).

29. W. D. Neff, J. E. Hind, Auditory thresholds of the cat. *J. Acoust. Soc. Am.* **27**, 480–483 (1955).

30. S. E. Currie, A. Boonman, S. Troxell, Y. Yovel, C. C. Voigt, Echolocation at high intensity imposes metabolic costs on flying bats. *Nat. Ecol. Evol.* **4**, 1174–1177 (2020).

31. D. J. Hartley, Stabilization of perceived echo amplitudes in echolocating bats. II. The acoustic behavior of the big brown bat, *Eptesicusfuscus*, when tracking moving prey. *J. Acoust. Soc. Am.* **91**, 1133–1149 (1992).

32. S. Hiryu, T. Hagino, H. Riquimaroux, Y. Watanabe, Echo-intensity compensation in echolocating bats (*Pipistrellus abramus*) during flight measured by a telemetry microphone. *J. Acoust. Soc. Am.* **121**, 1749–1757 (2007).

33. J. C. Koblitz, P. Stilz, W. Pflästerer, M. L. Melcón, H.-U. Schnitzler, Source level reduction and sonar beam aiming in landing big brown bats (*Eptesicus fuscus*). *J. Acoust. Soc. Am.* **130**, 3090–3099 (2011).

34. T. Budenz, A. Denzinger, H.-U. Schnitzler, Reduction of emission level in approach signals of greater mouse-eared bats (*Myotis myotis*): No evidence for a closed loop control system for intensity compensation. *PLOS ONE* **13**, e0194600 (2018).

35. L. Stidsholt, R. Müller, K. Beedholm, H. Ma, M. Johnson, P. T. Madsen, Energy compensation and received echo level dynamics in constant-frequency bats during active target approaches. *J. Exp. Biol.* **223**, jeb217109 (2020).

36. A. Denzinger, H.-U. Schnitzler, Echo SPL, training experience, and experimental procedure influence the ranging performance in the big brown bat, *Eptesicus fuscus*. *J. Comp. Physiol. A* **183**, 213–224 (1998).

37. K. R. Measor, B. C. Leavell, D. H. Brewton, J. Rumschlag, J. R. Barber, K. A. Razak, Matched behavioral and neural adaptations for low sound level echolocation in a gleaning bat, *Antrozous pallidus*. *eNeuro* **4**, ENEURO.0018-17 (2017).

38. S. Brinkløv, L. Jakobsen, J. M. Ratcliffe, E. K. V. Kalko, A. Surlykke, Echolocation call intensity and directionality in flying short-tailed fruit bats, *Carollia perspicillata* (*Phyllostomidae*). *J. Acoust. Soc. Am.* **129**, 427–435 (2011).

39. S. Brinkløv, E. K. V. Kalko, A. Surlykke, Dynamic adjustment of biosonar intensity to habitat clutter in the bat *Macrophyllum macrophyllum* (*Phyllostomidae*). *Behav. Ecol. Sociobiol.* **64**, 1867–1874 (2010).

40. M. Warnecke, W.-J. Lee, A. Krishnan, C. F. Moss, Dynamic echo information guides flight in the big brown bat. *Front. Behav. Neurosci.* **10**, 81 (2016).

41. K. Kugler, H. Luksch, H. Peremans, D. Vanderelst, L. Wiegrebe, U. Firzlaff, Optic and echo-acoustic flow interact in bats. *J. Exp. Biol.* **222**, jeb195404 (2019).

42. K. Egert-Berg, E. R. Hurme, S. Greif, A. Goldstein, L. Harten, L. G. Herrera, M. J. J. Flores-Martínez, A. T. Valdés, D. S. Johnston, O. Eitan, I. Borissov, J. R. Shipley, R. A. Medellin, G. S. Wilkinson, H. R. Goerlitz, Y. Yovel, Resource ephemerality drives social foraging in bats. *Curr. Biol.* **28**, 3667–3673.e5 (2018).

43. R. P. Wilson, M. P. Wilson, Dead Reckoning: A new technique for determining penguin movements at sea. *Meeresforschung.* **32**, 155–158 (1988).

44. R. P. Wilson, N. Liebsch, I. M. Davies, F. Quintana, H. Weimerskirch, S. Storch, K. Lucke, U. Siebert, S. Zankl, G. Müller, I. Zimmer, A. Scolaro, C. Campagna, J. Plötz, H. Bornemann, J. Teilmann, C. R. McMahon, All at sea with animal tracks; methodological and analytical solutions for the resolution of movement. *Deep Sea Res. II Top. Stud. Oceanogr.* **54**, 193–210 (2007).

45. R. J. Urick, *Principles of Underwater Sound* (Peninsula Pub, ed. 3, 1983).

46. K. Ghose, C. F. Moss, Steering by hearing: A bat's acoustic gaze is linked to its flight motor output by a delayed, adaptive linear law. *J. Neurosci.* **26**, 1704–1710 (2006).